Epithelial Barrier Integrity Profiling: Combined Approach Using Cellular Junctional Complex Imaging and Trans-Epithelial Electrical Resistance

Theresa J. Pell[1], Mike B. Gray[1], Sarah J. Hopkins[1], Richard Kasprowicz[1], James D. Porter[1], Tony Reeves[1], Wendy C. Rowan[1], Kuljit Singh[1], Ketil B. Tvermosegaard[1], Naheem Yaqub[2] and Gareth J. Wayne[1]

[1]GlaxoSmithKline R&D, Stevenage, Hertfordshire, SG1 2NY, UK

[2]University College London, London, NW3 2PF, UK

Corresponding author: Theresa J. Pell, GlaxoSmithKline R&D, Stevenage, Hertfordshire, SG1 2NY, UK. E-mail: theresa.j.pell@gsk.com

Keywords: human bronchial epithelial cells, barrier integrity, Trans-Epithelial Electrical Resistance, junctional complexes, high content imaging

Abstract

A core aspect of epithelial cell function is barrier integrity. A loss of barrier integrity is a feature of a number of respiratory diseases, including asthma, allergic rhinitis and chronic obstructive pulmonary disorder. Restoration of barrier integrity is a target for respiratory disease drug discovery. Traditional methods for assessing barrier integrity have their limitations. Trans-Epithelial Electrical Resistance (TEER) and dextran permeability methods can give poor *in vitro* assay robustness. Traditional junctional complex imaging approaches are labour intensive and tend to be qualitative, but not quantitative. To provide a robust and quantitative assessment of barrier integrity, high content imaging of junctional complexes was combined with TEER. A scalable immunofluorescent high content imaging technique, with automated quantification of junctional complex proteins zonula occludens-1 and occludin, was established in 3D pseudostratified primary human bronchial epithelial cells cultured at air-liquid interface. Ionic permeability was measured using TEER on the same culture wells.

The improvements to current technologies include: the design of a novel 24-well holder to enable scalable *in situ* confocal cell imaging without Transwell® membrane excision; the development of image analysis pipelines to quantify 'in-focus' junctional complex structures in each plane of a Z-stack; and the enhancement of the TEER data analysis process to enable statistical evaluation of treatment effects on barrier integrity. This novel approach was validated by demonstrating measurable changes in barrier integrity in cells grown under conditions known to perturb epithelial cell function.

Introduction

Epithelial barriers provide the first line of defence, protecting internal organs from the external environment. An intact and functional epithelial barrier is important for maintaining key biological functions of the respiratory epithelium.[1, 2] These functions include epithelial cell proliferation, differentiation, permeability and the production of pro-inflammatory mediators that modulate the respiratory airways immune response.[3] Airway epithelial barrier polarity and permeability are controlled by protein complexes which form tight junctions, adherens junctions and desmosomes between adjoining cells.[1] Tight junction complexes are located at the apical aspect of epithelium and control paracellular transport pathways between adjacent cells. They consist of scaffolding zonula occludens (ZO) proteins which connect transmembrane tight junction proteins, such as occludin and claudins, to the actin cytoskeleton, and junctional adhesion molecules. Adherens junctions, located lower in the epithelium, are formed by the transmembrane protein E-cadherin and catenin family proteins. Adherens junctions are key for cell-cell adhesion; they maintain cell polarization and regulate epithelial-mesenchymal transition (EMT). Desmosomes are located on the basolateral surface of the epithelium and connect to intermediate filaments.[1]

Epithelial barrier dysfunction is thought to play a significant role in several chronic respiratory illnesses including asthma[2, 4], allergic rhinitis[5, 6] and chronic obstructive pulmonary disease (COPD).[7] In asthma and allergic rhinitis, a defective epithelial barrier develops; in COPD, epithelial damage is caused by exposure to external irritants, such as cigarette smoke. Robust methods for assessing the formation and function of the epithelial barrier are needed for developing novel therapeutics for respiratory disorders.

Preclinical respiratory research primarily utilises a three dimensional (3D) *in vitro* Transwell® model consisting of primary human bronchial epithelial cells (HBECs) cultured at an air-liquid interface (ALI) on a semi-permeable membrane. This model is currently regarded as the gold-

standard *in vitro* model for studies of respiratory epithelium, with high predictive and face validity when compared to submerged HBEC or cell line-based ALI models, which lack key features of the respiratory tract *in vivo*.[8] HBECs are cultured to confluency in Transwell® inserts before the media is removed from the apical surface of the cells, exposing the cells to air. The cells are cultured over a period of 4-6 weeks, during which they undergo mucociliary differentiation into goblet, club and ciliated cell phenotypes forming a pseudostratified 3D epithelium. The formation of junctional complexes between adjacent cells in this model forms an *in vitro* epithelial barrier.

Several techniques have been developed to qualitatively or quantitatively characterise epithelial barrier integrity in ALI cultures. These include: tight junction complex protein visualization by microscopy; macromolecular permeability using labeled large molecular weight molecules, such as fluorescein isothiocyanate (FITC)-labeled dextrans; and ionic permeability by trans-epithelial or -endothelial electrical resistance (TEER).[9, 10] In this study, to achieve a combined approach to profiling epithelial barrier integrity, TEER and imaging of junctional complex proteins were selected as methodologies that could be used to generate complementary data from the same HBEC ALI culture well.

TEER is a non-invasive, real-time quantitative method for measuring barrier integrity in Transwell® culture models. The two main techniques typically used to measure TEER, in *in vitro* models, are the Ohm's Law electrical resistance method and impedance spectroscopy.[9, 11] A number of factors can affect assay robustness of TEER measurements including temperature, cell seeding density and culture time, media composition and shear stress.[9] When performing the Ohm's Law method using a voltohmmeter with a handheld "chopstick" electrode pair, variation can also be introduced by the positioning of the electrodes in the apical

and basolateral compartments of a Transwell® epithelial cell culture and by the potential for the electrodes to cause damage to the cell layer during measurement. All these factors need to be well controlled to minimise assay variability.[9]

Immunofluorescent imaging has also been used extensively in HBEC ALI cultures to determine ciliation and formation of junctional complexes.[12, 13, 14] ALI culture methodology has experienced some level of automation and scalability in recent years, such as incorporation of bioreactor culture mechanisms.[15] The fluorescent imaging methods used to evaluate *in vitro* ALI models remain labor intensive and lack automated image analyses to enable batch quantification. As a result, they offer poor scalability which has limited use in target validation studies and higher-throughput drug discovery. High magnification fluorescent microscopy protocols for 3D respiratory epithelium ALI cultures typically involve several manual steps. Cells are fixed, blocked and permeabilised within the Transwell® insert. Then the insert membranes are manually excised, prior to *in situ* immunolabelling of junctional complex proteins. Finally, the inserts are individually inverted and mounted onto coverslips for imaging. This method is required to allow visualization of cells growing at ALI with the high magnification lenses needed to image cilia or junctional complex proteins. Imaging of the 3D epithelium formed in HBEC ALI cultures can also be a challenging and time-consuming process because it requires layered, Z-plane confocal imaging to enable quantification.

We present a validated, systematic and scalable 3D quantitative immunofluorescent imaging technique to assess barrier integrity *in situ* within Transwell® inserts via the evaluation of junctional complex proteins (ZO-1 and occludin). For this purpose, a novel 3D-printed 24-well Transwell® holder was designed to enable scalable, *in situ*, high-magnification confocal imaging of Transwell® ALI cultures, without the need for membranes to be excised and

mounted. Cultures were imaged as a Z-stack and automated image analysis pipelines were established to identify and quantify junctional complexes from 'in-focus' planes of the 3D cultures.

We also present an improved data analysis process to evaluate changes in ionic permeability measured by TEER. We applied log10 transformation and calculated changes in barrier integrity as the change in log10(mean TEER) from basal or unstimulated control samples. This method enabled data analysis to be performed without the requirement of a blank well correction.

To validate this methodology, we performed two case studies. In the first, we reduced epithelial barrier integrity by culturing cells at a lowered seeding density and treated these epithelial layers with Transforming Growth Factor beta-1 (TGF-β1) to cause EMT, characterised by loss of cell-cell junctions.[16, 17] In the second study, epithelial layers were treated with the divalent cation chelator ethylenediaminetetraacetic acid (EDTA) which causes loss of cell-cell adhesion, via disruption of adherens junctions.[18]

This body of work improved the widely used immunofluorescent imaging and TEER methodologies to form a powerful analytical toolbox for epithelial barrier integrity analysis in Transwell® cultures. Combining measurement of paracellular ionic permeability with our imaging pipeline to assess junctional complex proteins, enables quantitative profiling of multiple barrier integrity parameters from the same HBEC ALI cultures. Our scalable method provides a valuable tool for respiratory drug discovery target validation studies.

Materials and Methods

Materials

All reagents were from Sigma-Aldrich (Gillingham, Dorset, UK), unless otherwise stated. UltraPure™ 0.5 M EDTA, pH 8.0 (Invitrogen 15575; Thermo Fisher Scientific, Waltham MA). TGF-β1 (HZ1011; Proteintech, Rosemont, IL) was prepared as a 5 µg/mL stock in MilliQ water containing 0.1% low endotoxin human serum albumin (A5843) and 4 mM HCl.

Cell Culture

Human biological samples used for this project were sourced ethically and their research use was in accordance with the terms of the informed consents.

For ***Study 1***, HBECs derived from two healthy, non-smoking donors (CC-2540; Lonza, Basel, Switzerland) were cultured following a method modified from Gray *et al.*[19] Briefly, cells were cultured in T75 cm^2 flasks in Bronchial Epithelial Growth Medium (BEGM™) (Lonza) for 6-7 days at 37°C / 5% CO_2, changing media and removing apical mucus every 2-3 days. Cells were lifted from flasks and seeded at 250,000, 125,000 or 75,000 cells/well onto individual Transwell® permeable membrane support inserts (6.5 mm diameter, 0.4 µm pore size, polystyrene membrane; Costar 3470; Corning Life Sciences, Tewksbury, MA) coated with 0.15 µg/ml human collagen type IV in a 24-well receiver plate (Costar 3524; Corning Life Sciences). Cells were cultured submerged for two days and then differentiated at the air-liquid interface for at least 21 days in Small Airway Epithelial Cell Basal Medium (SABM™) Differentiation Medium. For full cell culture methods, see Supplementary Materials.

For ***Study 2***, primary 3D human small airway epithelial layers, SmallAir™ (EP21; Epithelix, Geneva, Switzerland), from three healthy, non-smoker donors were used. Cells seeded at

300,000 cells/well were provided as ready-formed pseudostratified epithelial layers at post 28 days of differentiation. These ALI cultures were maintained until use, by changing SmallAir™ Culture Medium (EP64SA; Epithelix) and removing apical mucus, if required, every 2-3 days.

Cell Treatment

Once differentiated at ALI, cell cultures with TEER readings ≥300 Ω.cm^2 were considered to have formed an intact barrier.

Study 1: to demonstrate the effect of reducing cell number to suboptimal seeding densities, on the formation of an intact epithelial barrier, Lonza HBECs from one donor were seeded at 75,000, 125,000 or 250,000 cells/well. Cultures were treated daily, over a period of 72 h, with media vehicle control or 10 ng/mL TGF-β1 to disrupt epithelial barrier integrity in Bronchial Epithelial Basal Medium (BEBM™) Differentiation Medium (600 µL/well basolaterally, 20 µL/well apically). A time course was subsequently performed using cells from two donors seeded at 250,000 cells/well treated, in duplicate, daily for 72 h with basolateral (600 µL/well) 0.025% (v/v) DMSO vehicle control or TGF-β1 in SABM™ Differentiation Medium, as above (see **Fig. 1A** for workflow schematic). All differentiation media were supplemented with retinoic acid (50 nM) on the day of use.

Study 2: Epithelix SmallAir™ cultures seeded at 300,000 cells/well were treated with basolateral (600 µL/well) 0.025% DMSO vehicle control for 48 h or 1 mM EDTA for 1 h prior to the end of the 48 h incubation in SmallAir™ Culture Medium. Treatments were performed in triplicate, with replicates assayed on separate plates across two independent experiments.

TEER and Data Analysis

Each Transwell® ALI culture insert was placed into a well of a 24-well 'reservoir' receiver plate filled with pre-warmed unsupplemented 1:1 Small Airway Epithelial Cell Basal Medium (SABM™) (CC-3319; Lonza): Dulbecco's Modified Eagle Medium (DMEM) (Gibco 31966; Thermo Fisher Scientific) (600 µL/well). Apical surfaces of the epithelial layers were washed twice with pre-warmed medium (250 µL/well). The cultures were incubated submerged for 10 minutes in fresh pre-warmed medium, using the volumes above, at 37°C/5% CO_2. TEER was measured by the "chopstick" electrode method, either manually using a handheld Epithelial Voltohmmeter (EVOM) (EvoM2; World Precision Instruments, Sarosota, FL) or automatedly using an Automated TEER Measurement System with Corning HTS Transwell-24 (REMS-24) electrode (World Precision Instruments), according to the manufacturer's instructions. Triplicate readings were measured per well using the handheld probe; the automated system performs a single read per well.

For ***Study 1***, manual readings using the handheld probe were taken at 0 h before treatment and at 24, 48 and 72 h after vehicle control or TGF-β1 treatment in unsupplemented 1:1 SABM™:DMEM medium (250 µL/well). To minimize temperature fluctuations, Transwell® cultures in 24-well 'reservoir' plates were placed on a pre-warmed (37°C) Duolink In Situ Microplate Heat Transfer Block (DUO82065; Sigma-Aldrich) during TEER measurement. For ***Study 2***, using SmallAir™ cultures, automated TEER readings were taken on day 1, prior to vehicle control treatment. On day 3, TEER readings were taken 48 h after vehicle control treatment, and also before and after 1 h of 1 mM EDTA treatment.

A TEER data analysis pipeline was developed to enable statistical evaluation of treatment effects on barrier integrity. Resistance readings (Ω), without blank correction (see discussion), were multiplied by Transwell® insert membrane area to convert them to TEER ($\Omega.cm^2$).[9]

Triplicate technical replicate TEER reading values were averaged per well (mean TEER). Our assumptions are that within a well, error is normally distributed, reflecting the technical variation of the assay, and the variation between wells is log-normally distributed (see **Fig S3A** which illustrates heteroscedasticity between seeding densities), reflecting the biological variation between replicate wells. The within-well averages were log-transformed to ensure validity of downstream analysis (which assumes errors are normally distributed). The resulting endpoint, x, is defined in Eq. (1).

$$\text{Eq. (1):}\quad x = [\log10(\text{mean TEER})]$$

Data were plotted and analyzed as TEER change from baseline (Eq. (2)), calculated by subtracting the log10 transformed mean TEER at time 0 h ($TEER_0$) from the log10 transformed mean TEER at the time point of interest ($TEER_t$):

$$\text{Eq. (2):}\quad \Delta x_t = \log10(\text{mean } TEER_t) - \log10(\text{mean } TEER_0)$$

For the automated TEER system, measuring a single reading per well, log10(TEER) was substituted in place of log10(mean TEER) in the above equations.

Junctional Complex Immunostaining

Prior to fixation, HBEC ALI cultures in Transwell® inserts were gently washed three times with pre-warmed Phosphate Buffered Saline pH 7.4 supplemented with Ca^{2+}/Mg^{2+} (PBS), to remove mucus which can hinder immunostaining from the epithelial surface. Cells were fixed with 4% paraformaldehyde (Parafix; Pioneer Research Chemicals Ltd, Colchester, Essex, UK) for 15 minutes at room temperature and then washed three times with PBS. The apical epithelial surface was blocked and permeabilized with PBS containing 5% bovine serum albumin (BSA) and 0.5% Triton X-100 for 1 h at room temperature. After blocking and permeabilizing, primary antibodies against ZO-1 (1:100, 2.5 µg/mL final concentration; Invitrogen 61-73000;

Thermo Fisher Scientific) with or without occludin (1:100, 5 µg/mL; Invitrogen 33-1500; Thermo Fisher Scientific), were applied to the apical surface and incubated overnight at 4°C. Cells were washed for 5 minutes with PBS; this wash step was performed five times. Fluorescently conjugated Alexa Fluor® 488 (AF488) (1:500, 4 µg/mL; Molecular Probes A-21202; ThermoFisher Scientific) and Alexa Fluor® 647 (AF647) (1:500, 4 µg/mL; Molecular Probes A-31573; Thermo Fisher Scientific) anti-species secondary antibodies together with nuclear counterstain Hoechst 33342 (1.66 µM; Invitrogen H21492; Thermo Fisher Scientific), were applied to the apical surface for 1 h at room temperature. Cells were washed as described above and then transferred into PBS pH7.4 without Ca^{2+}/Mg^{2+} (PBS -/-) (D8537; Sigma-Aldrich) for imaging. For full method see Supplementary Materials.

High Content Image Acquisition

Cells were imaged, *in situ*, in Transwell® inserts using an IN Cell Analyzer 6000 (GE Healthcare Life Sciences, Little Chalfont, Buckinghamshire, UK) high content imager, by two methods. Firstly, widefield single plane images of Hoechst labeled nuclei at 10x magnification (0.45 numerical aperture (NA) air-objective) were captured, covering an area of 6656 x 6656 µm (25 fields of view per well in a five by five tiled square grid, without image overlap). These were used to generate a 'whole well' nuclei composite image to qualitatively assess cell coverage in the well, to provide additional context to the TEER values. Secondly, confocal Z-stacks (17 x 1.5 µm slices) of Hoechst labeled nuclei, ZO-1-AF647 and occludin-AF488 at 60x magnification (0.95 NA air objective), capturing six unique 222 x 222 µm fields of view per well, were used to assess junctional complexes (**Fig. 1B**). See Supplementary Materials **Table S1** for image acquisition settings.

For 10x magnification image acquisition, Transwell® inserts were suspended in a glass-bottomed 24-well SensoPlate™ (662892; Greiner Bio-One International GmbH, Kremsmünster, Austria) containing PBS -/- (600 µL/well) and covered with a plate lid which had black Nunc™ Sealing Tape (236703; Thermo Fisher Scientific) stuck to the underside.

To enable scalable *in situ* 60x confocal image acquisition of cells in Transwell® inserts without membrane excision, a 24-well holder was custom designed using SOLIDWORKS® 2019 (Dassault Systèmes SolidWorks Corporation, Waltham, MA) Computer Aided Design (CAD) software (**Fig. 2** and **Fig. S1**). The same footprint as a standard multi-well imaging plate was used to ensure compatibility with automated high content imaging platforms. The holder was 3D printed using Polyjet technology (Stratasys, Eden Prairie, MN) which uses a jetting technique similar to inkjet, but with a material that is curable by ultraviolet light. The Polyjet technology builds in 30-micron layers (Z axis) and will give an XY axes accuracy of approximately 50 microns, enabling production of a slot in the holder's base in which to slide coverglasses for the Transwell® inserts to sit on (**Fig. 2**). The holder was generated using VeroWhitePlus FullCure835 (Stratasys) which is a general purpose material ideal for this type of application. Two large (76 x 89 mm) size 2 coverglasses (L4381-2; Agar Scientific, Stansted, Essex, UK), the second one cut to size, were slid into the base of the holder.

For automated 60x magnification confocal imaging, laser and software auto-focusing did not reliably detect a defined aspect of the epithelium (e.g. cell nuclei or the Transwell® insert membrane). To avoid manual focusing of each Z-stack position, to ensure the full epithelial layer thickness was imaged, we performed a widefield 2D single plane exposure in the nuclei channel (without capturing an image) using laser auto-focus and a 50 µm software focus allowance. The focal plane of this exposure was used to set the focal point for each confocal

Z-stack, to enable automated imaging of junctional complexes. For ***Study 1***, to further aid auto-focusing, 1 µm blue FluoSpheres™ (Molecular Probes F8815; Thermo Fisher Scientific) were added to the apical surface (apical PBS was replaced with 100 µL/well of $2.4x10^8$ FluoSphere™ particles/mL in PBS -/-) and centrifuged for 1 min at 200 g to settle the fluorescent microspheres onto the epithelial surface. Transwell® inserts were transferred to the 3D printed holder, housing two coverglasses (size 2) in the base, retaining a bead of PBS -/- on the underside of each insert to make a liquid contact with the glass, to aid imaging (**Fig. 2C**).

Image Analysis

To characterise barrier integrity using cell-cell junctional complexes, we developed image analysis pipelines using Columbus™ v2.8.0 software (Perkin Elmer, Waltham, MA), to determine total junction protein area for occludin and ZO-1. To enable assay scalability, cells were imaged through the Transwell® membrane. This method resulted in high background fluorescence at lower planes, and for this reason, the 60x magnification Z-stack images were analyzed on a single plane basis, rather than as a maximum intensity projection (**Fig. 1C**. For details see Supplementary Materials **Fig. S2**). In brief, 'in-focus' junction protein area in each plane was identified by: i) performing sliding parabola background correction on the original image (AF488 channel for occludin; AF647 channel for ZO-1); ii) applying the ridge Spot Edge Ridge (SER) texture filter, to identify junctional complexes at cell boundaries; iii) using common threshold and size filters, to determine the image region; iv) clustering objects by distance and removing small objects, to identify regions of 'focused membrane'; and v) clustering of all 'focused membrane' objects, to calculate junction protein area summed for the six fields per well. The Columbus™ software reports the junction protein area separately for each plane; to achieve a total junction protein area for each well, the totals for each plane were summed using Microsoft® Excel (Microsoft® Office 365; Microsoft Corporation, Redmond,

WA). For each of the junction proteins measured, the image analysis process was the same, however, the sliding parabola background correction parameters were optimized (see Supplementary Materials **Tables S2-S4**). For EDTA treatment, total junction protein area was normalised to the number of fields in focus, due to one well failing to focus for one field. Junction protein total area data were square root-transformed because the variance increased with the magnitude of the response. A square root transformation achieved better stabilization of variance, i.e. ensured constant variance for all observations, than log10 transformation.

Statistical Analysis

Where appropriate, statistical analyses were performed using R version 2019[20] and R-package emmeans version 1.4.2[21]; no data for conditions tested were excluded from these analyses. Graphs were plotted using tidyverse[22] which is a collection of R packages for data science.

Prior to statistical analysis, TEER or mean TEER data were log10-transformed and junction complex protein data square root-transformed to stabilize variation.

For ***Study 1***, we performed one-way ANOVA to test whether TEER changes from baseline for wells with reduced seeding density or TGF-β1 treatment were significantly different to the change from baseline for vehicle controls. We used a separate one-way ANOVA for each treatment-control comparison. To analyse changes in TEER over time, a separate one-way ANOVA was fitted to the data for each timepoint. The *p*-values from these separate analyses will be correlated and thus do not carry the same weight that three independent *p*-values would. To test whether ZO-1 tight junction total protein area changes from baseline following TGF-β1 treatment were significantly different to the change from baseline for vehicle controls, we

fitted a general linear model to the ZO-1 data with two fixed effects: treatment and donor. This model differs from a two-way ANOVA in that it has no interaction terms.

For ***Study 2*,** to test whether TEER or ZO-1 total area changes from baseline following EDTA treatment were significantly different to the change from baseline for vehicle controls, we fitted general linear models with three fixed effects: treatment, HBEC donor and assay plate. This model differs from a three-way ANOVA in that it has no interaction terms.

Results

Automated Imaging and Quantification of Tight Junction Proteins

To enable evaluation of respiratory epithelial barrier integrity at sufficient scale for drug discovery, we developed an automated image acquisition and analysis pipeline to quantify tight junction proteins (**Figs. 1** and **S2**). We designed and 3D printed a 24-well holder to enable scalable, automated high magnification confocal imaging of HBEC ALI cultures *in situ* within Transwell® inserts (**Figs. 2** and **S1**). This negated the need to manually excise each insert membrane and mount them on coverslips, which is the method typically employed for high magnification confocal imaging of such epithelial layers.

Development of an Improved TEER Data Analysis Methodology

For these studies, we measured TEER using the Ohm's Law method. An alternating current (AC) is applied using a "chopstick" electrode pair inserted into the apical and basolateral compartments of a Transwell® epithelial cell culture. The measurement of electrical resistance, in Ohms (Ω), across the cell layer, is indicative of its paracellular permeability to ions and is proportional to the integrity of the epithelial barrier.[9, 11] To determine changes in ionic

permeability of the epithelial barrier, we developed an improved TEER data analysis process. TEER values are typically corrected by subtraction of a blank well containing the Transwell® insert semi-permeable membrane without cells, to determine the resistance of the epithelium.[9] Changes in TEER are often calculated as a percentage of the basal reading or unstimulated controls[23, 24, 25, 26]; however, percentage changes do not typically follow a normal distribution. We applied log10 transformation and calculated changes in barrier integrity as the change in log10(mean TEER) or log10(TEER) from baseline or untreated control (see Supplementary Materials **Tables S5-S8**). This method enabled data analysis to be performed without the requirement of blank well correction. TEER analyses from the two case studies used to validate this methodology will be presented in more detail in the following sections.

Development of a Combined TEER and Imaging Approach to Evaluate Barrier Integrity

TEER assay robustness can suffer from high variability due to environmental conditions and epithelium damage due to manual interventions during ALI culture. For ***Study 1*** we used the handheld EVOM "chopstick" electrode system, for which electrode positioning and epithelium damage caused by manual TEER measurement, can also affect assay robustness. We used 'whole well' nuclei imaging, to provide additional contextual information, to understand the TEER data. For example (see **Fig. 3A**), 10 ng/ml TGF-β1 reduced ionic permeability (mean TEER) whilst retaining good cell coverage, when seeded at 250,000 cells/well; this indicated treatment led to a loss of barrier integrity, without significant cell loss. In contrast, when cells were seeded at the suboptimal densities of 125,000 and 75,000 cells/well, the observed reductions in mean TEER were associated with visible gaps in the epithelial layer.

We combined measurement of paracellular ionic permeability with quantitative assessment of junctional complex proteins, to enable evaluation of multiple barrier integrity mechanisms from the same epithelial ALI cultures using the workflow described in **Fig. 1A**. For example,

daily treatment for 72 h of HBEC ALI cultures with 10 ng/mL TGF-β1 caused visible disruption to the ZO-1 and occludin tight junction protein 'honeycomb' pattern of staining, typical of an intact epithelial barrier (**Fig. 3B**). We quantified this change in barrier integrity by developing image analysis pipelines using Columbus™ software. The total area of junctional complex proteins occludin and ZO-1, were calculated within 'in-focus' planes of the epithelium for each well (see **Fig. 3C** for exemplar images showing identification of 'in-focus' ZO-1 area).

Validation of Quantitative Combined TEER and Imaging Approach

To validate and assess assay robustness of our quantitative combined TEER and imaging approach for evaluating bronchial epithelial barrier integrity, we performed two studies, employing differing methods, to reduce barrier integrity. The first study used epithelial cultures differentiated at ALI, from two Lonza healthy, non-smoker primary HBEC donors, using suboptimal seeding densities and induction of EMT with TGF-β1 to reduce barrier integrity.[16, 17] The second study used Epithelix healthy, non-smoker primary SmallAir™ cultures from three donors, provided as pseudostratified epithelial layers. These cells were treated with EDTA which chelates divalent cations (e.g. Ca^{2+}), resulting in loss of cell-cell adhesion. The presence of calcium is required to achieve the correct conformation, to allow E-cadherin proteins on neighboring cells to bind to each other, to form an adherens junction.[18]

The majority of the epithelial layers used in both studies had formed a good intact barrier (mean TEER >300 $\Omega.cm^2$); baseline mean TEER values are shown in **Fig S3**. See Supplementary Materials **Tables S5-S12** for full TEER and junction complex protein total area data and statistical analyses.

Study 1. To assess the effects of seeding density on epithelial barrier integrity, we seeded 250,000, 125,000 or 75,000 cells/well in BEGM™ and then differentiated them at ALI in SABM™ Differentiation Medium. Typically, 250,000-300,000 cells/well are seeded into 6.5 mm diameter Transwell® inserts to generate an intact epithelial barrier; 125,000 and 75,000 cells/well were considered suboptimal seeding densities. As expected, we observed a progressive increase in newly formed intact epithelial barrier with increasing seeding density; measured by both ionic permeability (increasing log10(mean TEER); **Fig. 4A**) and amount of junctional complex proteins (increased occludin and ZO-1 total area by confocal immunofluorescent imaging; **Fig. 4B**).

We also observed reductions in barrier integrity, as expected, after daily treatment over the course of 72 h with 10 ng/ml TGF-β1 to induce EMT, characterised by loss of cell-cell junctions. Log10(mean TEER) (**Fig. 4C**) and tight junction protein (occludin and ZO-1) total area (**Fig. 4D**) were reduced at all seeding densities. A time-dependent loss of barrier integrity (negative TEER Change) was also demonstrated following TGF-β1 treatment over 72 h, using 250,000 cells/well cultures for both donors (**Fig. 4E**). At the end of the time course, these cells also had reduced tight junction protein area (**Fig. 4F**).

Study 2. To further validate this improved methodology, we assessed the effect of 1 h treatment with 10 mM EDTA on SmallAir™ HBEC ALI cultures seeded at 300,000 cells/well. EDTA chelates calcium and is expected to reduce barrier integrity by interfering with cell-cell adhesion. We observed an approximate 4-fold reduction in ionic permeability measured by TEER (**Fig. 5A**) and a 6-fold reduction in the amount of ZO-1 tight junction complex protein total area (**Fig. 5B**).

In summary, data from these validation studies, demonstrated that barrier integrity reductions caused by suboptimal HBEC seeding densities or treatment of epithelial layers with agents that disrupt cell-cell junctions, were quantifiable using our combined approach of improved TEER data analysis and automated tight junction protein image analysis.

Discussion

Integrated measurement of ionic permeability and junctional complex protein interactions within the same sample, provides a more robust method for assessing epithelial barrier integrity compared to using either assessment alone by providing complementary information. Epithelial macromolecular flux, resulting from changes in junctional complex structure or function, can increase without an associated drop in ionic permeability measured by TEER, highlighting the importance of using multiple approaches to assess barrier integrity.[10] Our method can be applied to multiple stages of the drug discovery process for analysis of 100-1000 samples, including target validation studies, compound screening and safety assessment.

Study 1 used two independent donors to develop this combined TEER and quantitative imaging approach for barrier integrity profiling. This methodology was further validated by applying it to ***Study 2*** using an additional three independent donors, with triplicate wells per condition, to capture donor-to-donor variability. This work used a total of five independent donors; we have demonstrated this methodology works across the five individual donors from two different sources, providing confidence that it is a reproducible technique for evaluating barrier integrity.

TEER Ohm's Law method is a well-established technique which uses electrodes placed in medium on either side of the cell barrier and an alternating current. Measuring the voltage and current enables the resistance to be calculated; the more intact the barrier, the higher the

resistance. Both the maintenance of ALI cell cultures requiring removal of secreted mucus and the TEER technique itself, require a high level of dexterity to minimise damage to the epithelial cell layer. By imaging the whole well, it is possible to assess whether reductions in TEER are truly indicative of loss of barrier integrity through increased ionic permeability, and not due to cell loss through inadvertent damage of cell cultures, or cell death.

For analysis purposes, an enhanced novel TEER data analysis process was performed. TEER data was log10-transformed, enabling statistical evaluation of treatment effects on barrier integrity using a change in log10(mean TEER) from baseline. Typically, TEER values are corrected using a blank well, containing the Transwell® insert semi-permeable membrane without cells, to determine the resistance of the epithelium.[9] TEER changes are often calculated as a percentage of the basal reading (time 0 h) or unstimulated controls[23, 24, 25, 26]; however, percentage changes do not typically follow a normal distribution. The new methodology described here, using change in log10(mean TEER), enables statistical evaluation of treatment effects on barrier integrity, while avoiding assuming normality of % change in mean TEER values (ratios of observations are generally not normally distributed). In addition, this TEER data analysis method, using log10 transformation, negated the need for blank well correction, typically employed when calculating TEER by traditional methods.[9] Under the assumption that the expected blank well value does not depend on time, change in log10(mean TEER) or log10(TEER) is mathematically independent of the expected blank well value. Specifically, if the expected blank well value is log10(mean $TEER_B$) and assumed known, then the blank well corrected observation is given by Eq. (3).

$$\text{Eq. (3):}\quad x_t = \log10(\text{mean } TEER_t) - \log10(\text{mean } TEER_B)$$

Change in blank well corrected log10(mean TEER) would be given by Eq. (4), where the last expression is independent of log10(mean $TEER_B$).

Eq. (4): $\Delta x_t = (\log10(TEER_t) - \log10(TEER_B)) - (\log10(TEER_0) - \log10(TEER_B))$

$= \log10(\text{mean } TEER_t) - \log10(\text{mean } TEER_0)$

Ideally for blank correction, the blank semi-permeable membrane should be surface treated in the same manner as those used to grow the epithelial layers. This TEER analysis method was also implemented for epithelium bought as pre-formed ALI pseudostratified epithelial layers; setting up blank wells for such cultures is challenging because the Transwell® insert coating methods may be proprietary and blank wells may not be supplied. In instances where it is not possible to generate a true blank well, the ability to forego the need for blank correction is an important consideration.

This technique of combining TEER with 'whole-well' nuclei imaging, adds context to losses in barrier integrity measured by ionic permeability. It highlights marked cell loss resulting from cytotoxicity or significant mechanical disruption during ALI cell culture / TEER measurement, which may cause reductions in barrier integrity independent of cell treatment.

Visualizing tight junctions of epithelial cells cultured at ALI *in situ*, requires high magnification (60x) confocal imaging using lenses which typically have working distances too short to image cells *in situ* on Transwell® membranes suspended within standard 24-well imaging plates. We achieved this using the IN Cell Analyzer 6000 combined with a custom made 3D printed 24-well holder to accommodate the Transwell® inserts. This avoids the need to excise the membranes, with attached cells, from the Transwells® and to mount them onto coverslips for imaging work. This minimises damage through manual manipulation and significantly speeds up data acquisition. For ***Study 1***, fluorescent FluoSpheres™ were settled onto the epithelial surface to aid microscope auto-focusing, to avoid the need to manually focus each well. For subsequent studies, including ***Study 2***, depending on the nature of the epithelial

culture, it was not always necessary to apply FluoSpheres™ to aid auto-focusing. A consistent approach was taken within each study.

The challenge with studying junctional complex protein interactions, is that the junctions lie in different planes of view, due to the fact that the cells do not grow in a uniform layer. This requires taking multiple confocal planes of view, to form a Z-stack. Typically, Z-stacks would be analysed as a maximum intensity projection image. In order to improve scalability of the technique, by removing the necessity to excise Transwell® membrane inserts and mount them on coverslips, the cells were imaged through the Transwell® insert membrane. This technique resulted in a high fluorescence background in Z-stack planes close to the insert membrane. To overcome this, the Z-stacks were analysed plane-by-plane. To analyse the cell-cell junctions, image analysis algorithms were developed to quantify 'in-focus' junctional complex structures in each Z plane. This helps to overcome bias in data analysis incurred when a subjective analysis of stained images is undertaken. One limitation of this image analysis methodology, is that the same object can be counted in multiple planes; the error would be consistent between samples when using this method to analyse epithelial layers of similar thickness, mitigating its impact on experimental analysis. Ideally, the epithelial layer would be analysed as a 3D object; for example, the amount of tight junction protein could be analysed as a volume or a 3D surface. Currently, there is a lack of off-the-shelf 3D image analysis software applicable for use with a wide range of high content imaging platforms and that is suitable for automated batch analysis of multi-well data at the scales required for drug discovery.[27] Whilst the studies presented here assessed occludin and ZO-1, this image analysis pipeline could be modified to evaluate other junctional complex proteins, such as E-cadherin and claudins.

To the best of our knowledge this is the first report of using a combined TEER and quantitative imaging approach for assessment of epithelial barrier integrity. It has been successfully applied to a drug discovery target validation project within GlaxoSmithKline to investigate whether target modulation adversely affected respiratory epithelial barrier integrity. It has the potential to be used for other epithelial barriers of interest, for example, impaired gastrointestinal epithelial barrier integrity is associated with inflammatory bowel disease, obesity and fatty liver diseases.[28] The technique could also be further scaled to a 96-well plate format.

Declaration of Conflicting Interests

The authors declared no potential conflicts of interest with respect to the research, authorship, and/or publication of this article.

Funding

The authors received no financial support from any funding agency in the public, commercial, or not-for-profit sectors for the research, authorship and/or publication of this article.

Acknowledgements

Perkin Elmer for Columbus™ image analysis software guidance.

References

1. Brune, K.; Frank, J.; Schwingshackl, A.; et al. Pulmonary Epithelial Barrier Function: Some New Players and Mechanisms. *Am. J. Physiol.: Lung Cell. Mol. Physiol.* **2015,** *308*, L731-45.
2. Gon, Y.; Hashimoto, S. Role of Airway Epithelial Barrier Dysfunction in Pathogenesis of Asthma. *Allergol. Int.* **2018,** *67*, 12-17.

3. Nawijn, M. C.; Hackett, T. L.; Postma, D. S.; et al. E-Cadherin: Gatekeeper of Airway Mucosa and Allergic Sensitization. *Trends Immunol.* **2011,** *32,* 248-55.
4. Xiao, C.; Puddicombe, S. M.; Field, S.; et al. Defective Epithelial Barrier Function in Asthma. *J. Allergy Clin. Immunol.* **2011,** *128,* 549-56 e1-12.
5. Steelant, B.; Wawrzyniak, P.; Martens, K.; et al. Blocking Histone Deacetylase Activity as a Novel Target for Epithelial Barrier Defects in Patients with Allergic Rhinitis. *J Allergy Clin Immunol* **2019,** *144,* 1242-1253 e7.
6. Georas, S. N. Targeting Histone Deacetylases to Restore Epithelial Barrier Integrity: A New Option for Personalized Medicine in Patients with Allergic Airway Disorders? *J Allergy Clin Immunol* **2019,** *144,* 1172-1174.
7. Aghapour, M.; Raee, P.; Moghaddam, S. J.; et al. Airway Epithelial Barrier Dysfunction in Chronic Obstructive Pulmonary Disease: Role of Cigarette Smoke Exposure. *Am. J. Respir. Cell Mol. Biol.* **2018,** *58,* 157-169.
8. Upadhyay, S.; Palmberg, L. Air-Liquid Interface: Relevant in Vitro Models for Investigating Air Pollutant-Induced Pulmonary Toxicity. *Toxicol. Sci.* **2018,** *164,* 21-30.
9. Srinivasan, B.; Kolli, A. R.; Esch, M. B.; et al. Teer Measurement Techniques for in Vitro Barrier Model Systems. *J. Lab. Autom.* **2015,** *20,* 107-26.
10. Rezaee, F.; Georas, S. N. Breaking Barriers. New Insights into Airway Epithelial Barrier Function in Health and Disease. *Am J Respir Cell Mol Biol* **2014,** *50,* 857-69.
11. Benson, K.; Cramer, S.; Galla, H. J. Impedance-Based Cell Monitoring: Barrier Properties and Beyond. *Fluids Barriers CNS* **2013,** *10,* 5.
12. Hardyman, M. A.; Wilkinson, E.; Martin, E.; et al. TNF-Alpha-Mediated Bronchial Barrier Disruption and Regulation by Src-Family Kinase Activation. *J Allergy Clin Immunol* **2013,** *132,* 665-675 e8.

13. Rayner, R. E.; Makena, P.; Prasad, G. L.; et al. Optimization of Normal Human Bronchial Epithelial (NHBE) Cell 3D Cultures for In Vitro Lung Model Studies. *Sci Rep* **2019,** *9*, 500.
14. Marrazzo, P.; Maccari, S.; Taddei, A.; et al. 3D Reconstruction of the Human Airway Mucosa In Vitro as an Experimental Model to Study NTHi Infections. *PLoS One* **2016,** *11*, e0153985.
15. Aufderheide, M.; Forster, C.; Beschay, M.; et al. A New Computer-Controlled Air-Liquid Interface Cultivation System for the Generation of Differentiated Cell Cultures of the Airway Epithelium. *Exp. Toxicol. Pathol.* **2016,** *68*, 77-87.
16. Xu, J.; Lamouille, S.; Derynck, R. TGF-Beta-Induced Epithelial to Mesenchymal Transition. *Cell Res.* **2009,** *19*, 156-72.
17. Hackett, T. L.; Warner, S. M.; Stefanowicz, D.; et al. Induction of Epithelial-Mesenchymal Transition in Primary Airway Epithelial Cells from Patients with Asthma by Transforming Growth Factor-Beta1. *Am. J. Respir. Crit. Care Med.* **2009,** *180*, 122-33.
18. Bhatt, T.; Rizvi, A.; Batta, S. P.; et al. Signaling and Mechanical Roles of E-Cadherin. *Cell Commun Adhes* **2013,** *20*, 189-99.
19. Gray, T. E.; Guzman, K.; Davis, C. W.; et al. Mucociliary Differentiation of Serially Passaged Normal Human Tracheobronchial Epithelial Cells. *Am. J. Respir. Cell Mol. Biol.* **1996,** *14*, 104-12.
20. R Core Team R: A Language and Environment for Statistical Computing. https://www.R-project.org/ (accessed August 31, 2020).
21. Lenth, R. Emmeans: Estimated Marginal Means, Aka Least-Squares Means. https://CRAN.R-project.org/package=emmeans (accessed August 31, 2020).

22. Wickham, H.; Averick, M.; Bryan, J.; et al. Welcome to the Tidyverse. *Journal of Open Source Software* **2019,** *4*.
23. Sedgwick, J. B.; Menon, I.; Gern, J. E.; et al. Effects of Inflammatory Cytokines on the Permeability of Human Lung Microvascular Endothelial Cell Monolayers and Differential Eosinophil Transmigration. *J Allergy Clin Immunol* **2002,** *110*, 752-6.
24. Balogh Sivars, K.; Sivars, U.; Hornberg, E.; et al. A 3D Human Airway Model Enables Prediction of Respiratory Toxicity of Inhaled Drugs In Vitro. *Toxicol Sci* **2018,** *162*, 301-308.
25. Clark, P. R.; Kim, R. K.; Pober, J. S.; et al. Tumor Necrosis Factor Disrupts Claudin-5 Endothelial Tight Junction Barriers in Two Distinct NF-KappaB-Dependent Phases. *PLoS One* **2015,** *10*, e0120075.
26. Rezaee, F.; Meednu, N.; Emo, J. A.; et al. Polyinosinic:Polycytidylic Acid Induces Protein Kinase D-Dependent Disassembly of Apical Junctions and Barrier Dysfunction in Airway Epithelial Cells. *J Allergy Clin Immunol* **2011,** *128*, 1216-1224 e11.
27. Booij, T. H.; Price, L. S.; Danen, E. H. J. 3D Cell-Based Assays for Drug Screens: Challenges in Imaging, Image Analysis, and High-Content Analysis. *SLAS Discov* **2019,** *24*, 615-627.
28. Lee, B.; Moon, K. M.; Kim, C. Y. Tight Junction in the Intestinal Epithelium: Its Association with Diseases and Regulation by Phytochemicals. *J Immunol Res* **2018,** *2018*, 2645465.

Figure Legends

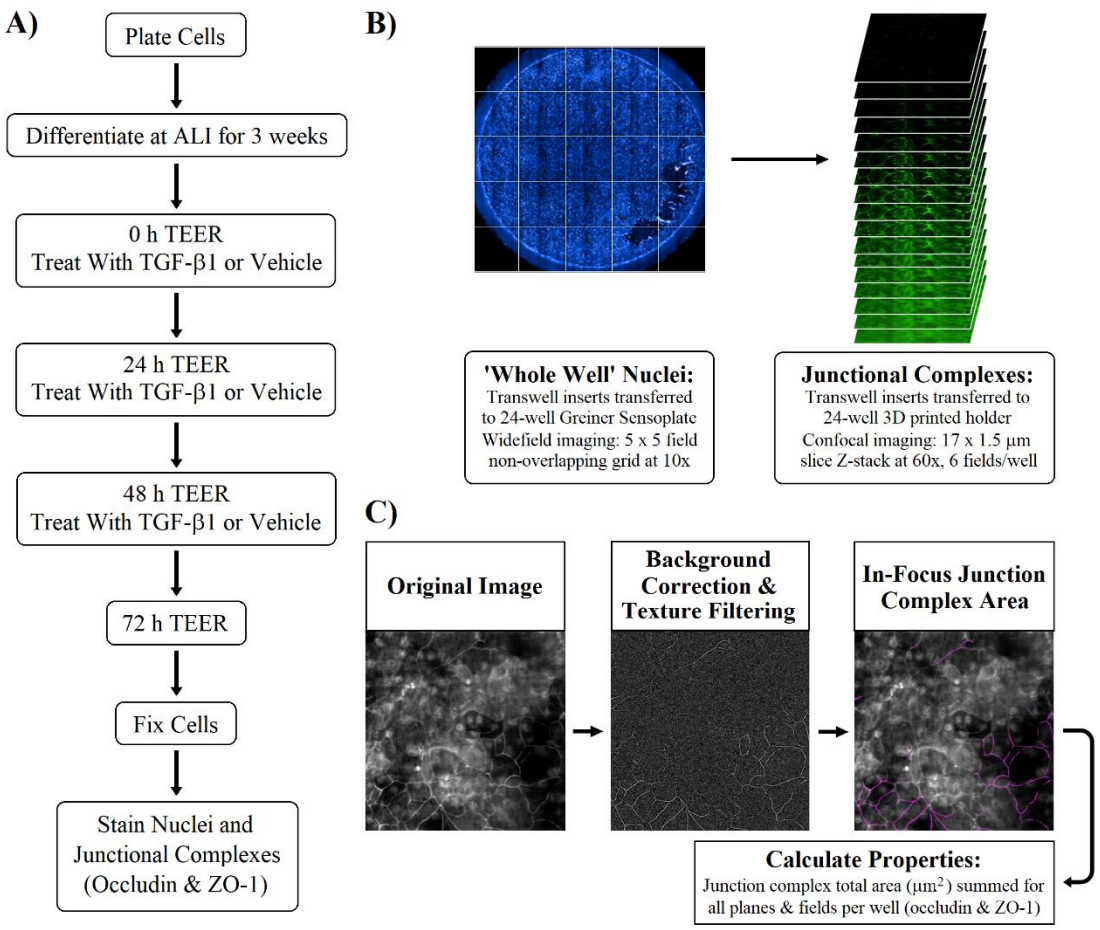

Figure 1. Combined TEER and junctional complex high content imaging approach to profile HBEC barrier integrity. (**A**) Schematic of the experimental workflow. (**B**) Schematic of the image acquisition workflow. (**C**) Schematic of the image analysis and quantification pipeline, using Columbus™ software, demonstrating identification of 'in focus' junction protein area. Occludin and ZO-1 'in-focus' areas were summed for all planes and fields per well, to give a total junctional complex protein area. Exemplar segmented images are shown for ZO-1. Further details are available in the Supplementary Materials.

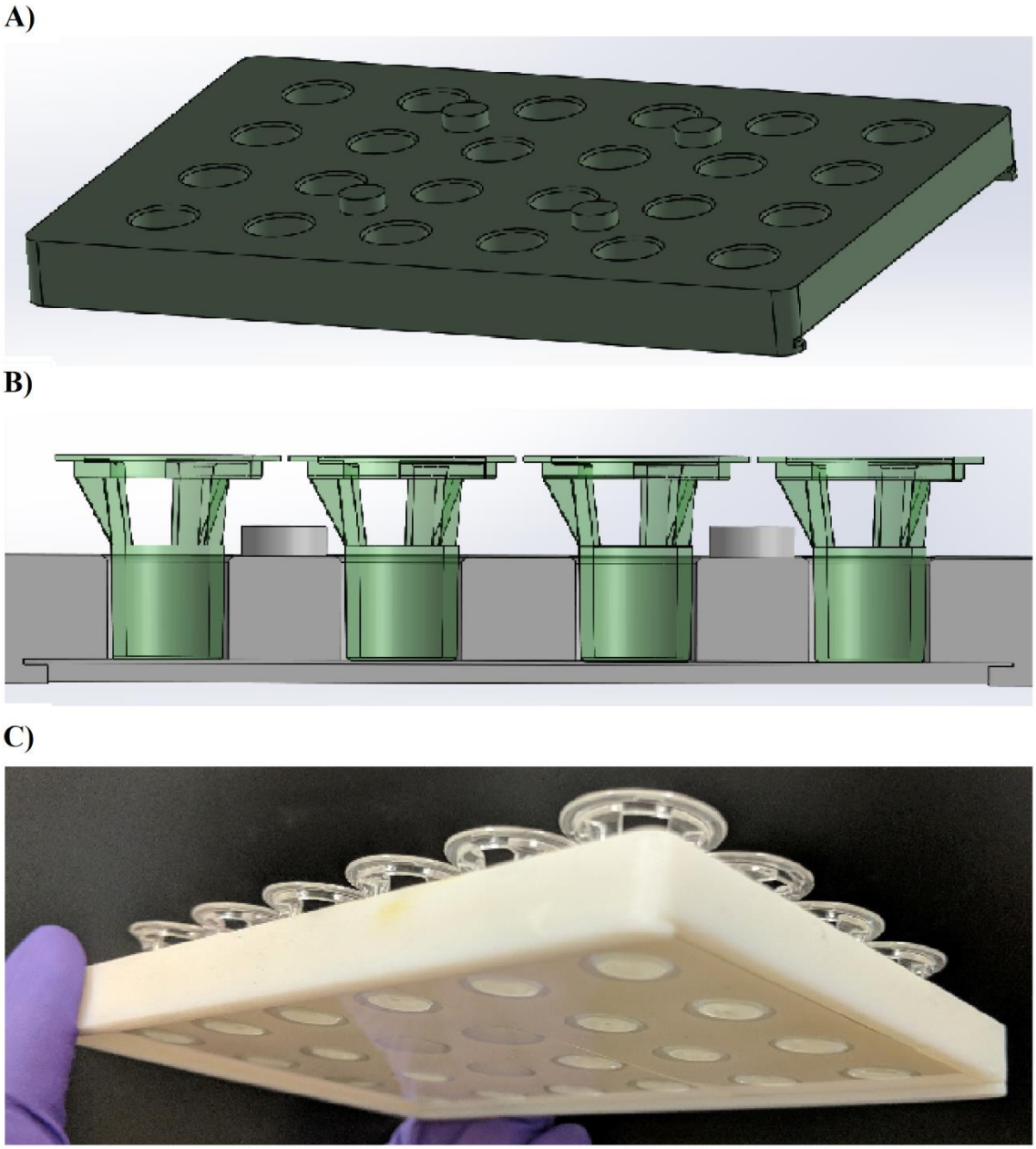

Figure 2. 3D printed 24-well Transwell® insert holder designed to the same footprint as a standard multi-well imaging plate, to ensure compatibility with automated high content imaging platforms. SOLIDWORKS® 2019 CAD designs (full specifications are provided in Supplementary Materials **Fig. S1**): (**A**) Top view of the holder measuring 127.8 mm (length) x 85.5 mm (width) x 10.4 mm (height); and (**B**) Internal view showing location of the Transwell® inserts and slot in the holder's base for the coverglasses. (**C**) Photograph of the 3D printed holder containing Transwell® inserts located on the No.2 coverglasses.

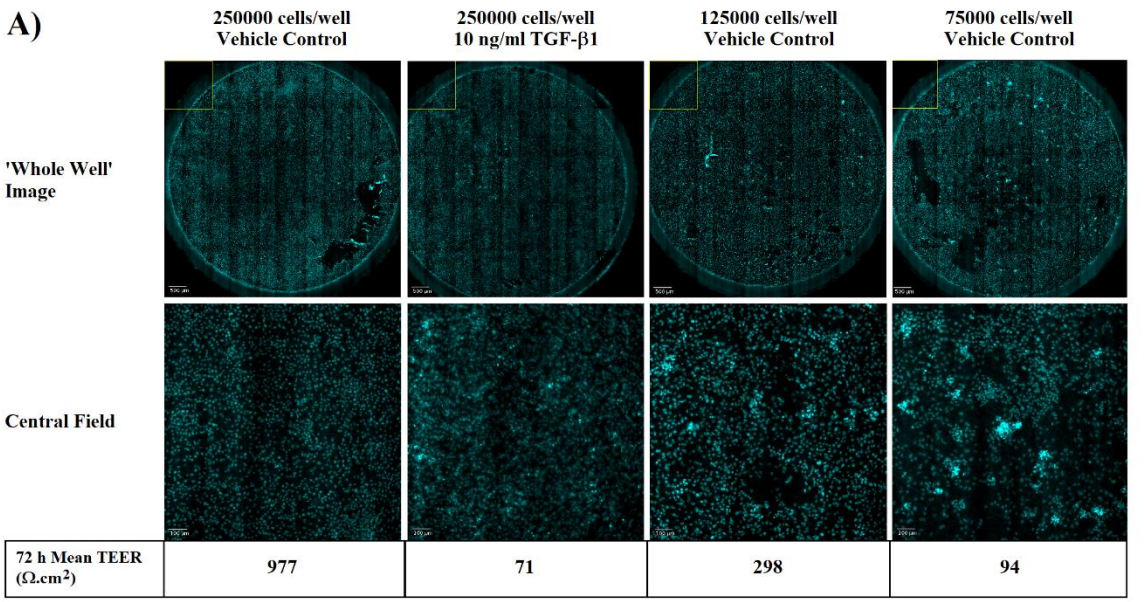
A)
250000 cells/well
Vehicle Control
250000 cells/well
10 ng/ml TGF-β1
125000 cells/well
Vehicle Control
75000 cells/well
Vehicle Control
'Whole Well'
Image
Central Field
72 h Mean TEER
(Ω.cm²)
977
71
298
94

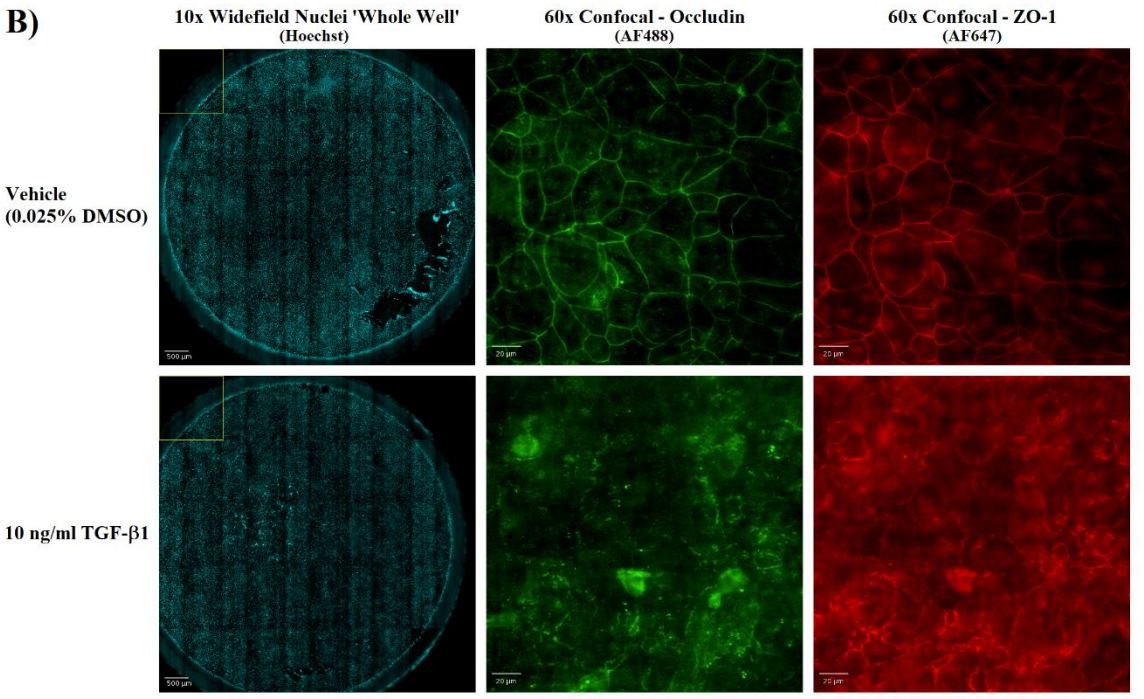
B)
10x Widefield Nuclei 'Whole Well'
(Hoechst)
60x Confocal - Occludin
(AF488)
60x Confocal - ZO-1
(AF647)
Vehicle
(0.025% DMSO)
10 ng/ml TGF-β1

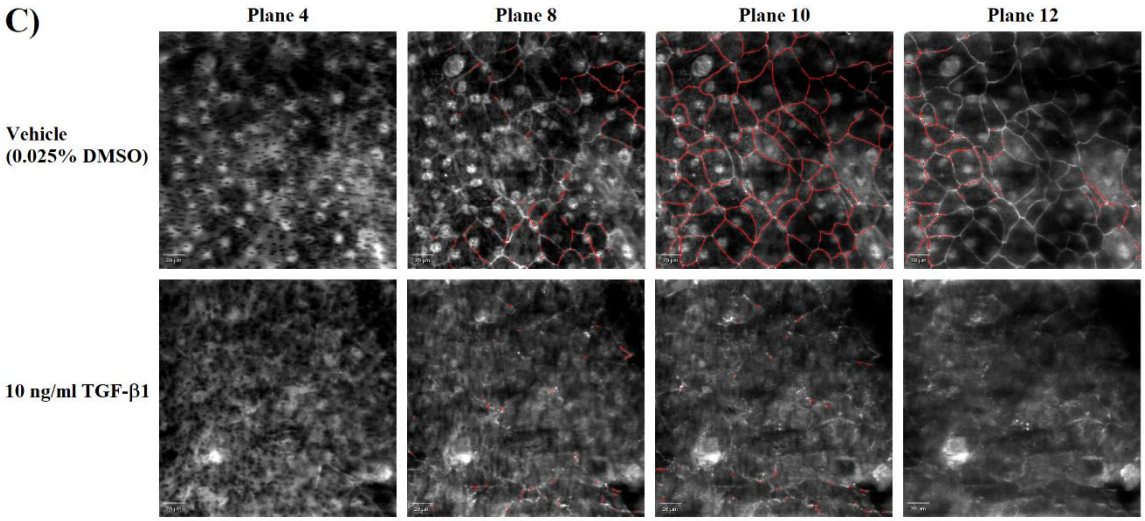
C)
Plane 4
Plane 8
Plane 10
Plane 12
Vehicle
(0.025% DMSO)
10 ng/ml TGF-β1

Figure 3. Junctional complex protein imaging. Disruption of occludin and ZO-1 junctional complexes by daily treatment of Lonza HBEC ALI cultures with 10 ng/mL TGF-β1 for 72 h to induce EMT. (**A**) Exemplar 10x magnification 'whole well' and central field nuclei images with their corresponding 72 h mean TEER values. Imaging provides additional contextual information to aid understanding of TEER data. In these examples, TGF-β1 reduces ionic permeability (mean TEER) without altering cell number, whereas for 125,000 and 75,000 cells/well fields, the reduction in mean TEER was associated with gaps in the epithelial layer. (**B**) Representative 10x magnification widefield nuclei images of the 'whole well' and 60x magnification confocal images, showing maximum projections of four planes, for occludin and ZO-1. TGF-β1 disruption of barrier integrity was demonstrated by a loss of occludin and ZO-1 'honeycomb' pattern of staining, indicative of an intact epithelial barrier. (**C**) Exemplar image analysis showing identification of ZO-1 tight junctions, highlighted in red, in 'in-focus' planes of the Z-stack.

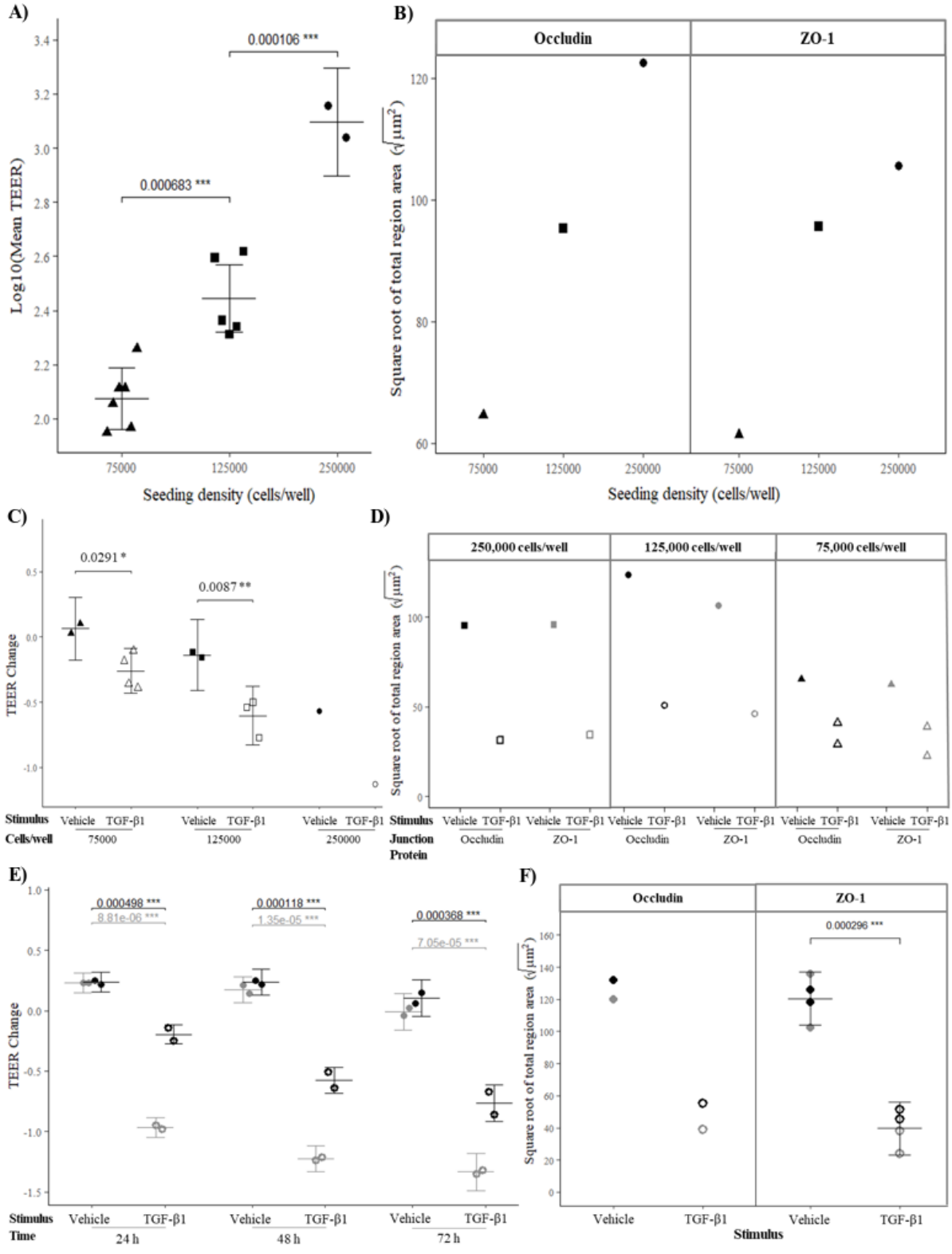

Figure 4: ***Study 1*** – lowering cell seeding density and daily treatment for up to 72 h with 10 ng/mL TGF-β1 (open symbols), to induce EMT, impaired epithelial barrier integrity in Lonza healthy, non-smoker primary HBEC ALI cultures. This was demonstrated by reduced ionic

permeability (TEER) and total area of junctional complex proteins (occludin and ZO-1 imaging) in two independent experiments. *Experiment 1*: a progressive increase in newly formed intact epithelial barrier was observed with increasing seeding density measured by basal 0 h log10(mean TEER) (**A**) and vehicle control junctional complex protein total area (**B**). TGF-β1 treatment for 72 h disrupted ionic permeability (negative TEER change; **C**) and junctional complexes (**D**) at all seeding densities. Cells were seeded at 75,000 (triangles), 125,000 (squares) and 250,000 cells/well (circles). Wells were treated with vehicle control (closed symbols) or TGF-β1 (open symbols). *Experiment 2*: a time-dependent loss of barrier integrity (negative TEER Change) was observed for both donors following treatment with TGF-β1 (**E**); donor two (gray circles) had a more pronounced TEER change than donor one (black circles). At 72 h, loss of junctional complex protein total area was similar for both donors (**F**). Individual data points with treatment mean +/- 95% confidence intervals are plotted. Statistical analysis by one-way ANOVA (**A**, **C** & **E**) or general linear model (**F**) with *p*-values: $*p < 0.05$, $**p < 0.01$ and $***p < 0.001$. Separate one-way ANOVAs were fitted per treatment-control comparison (**A** & **C**) or per timepoint (**E**).

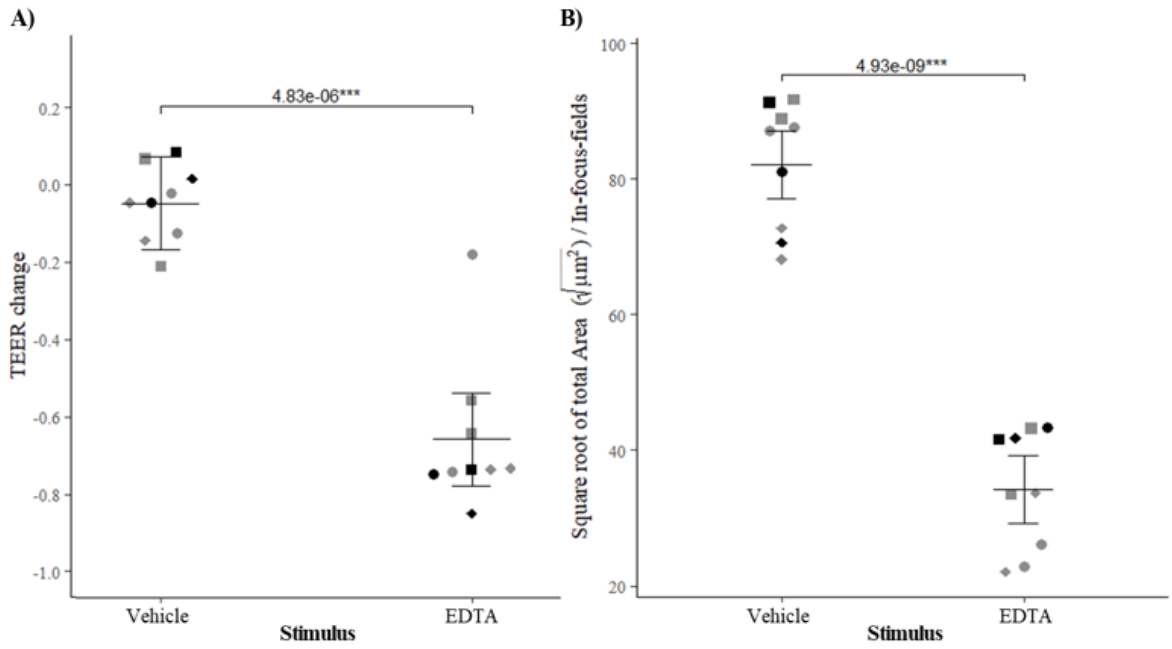

Figure 5: ***Study 2*** – epithelial barrier integrity was disrupted in primary healthy, non-smoker SmallAir™ HBEC cultures by 1 h treatment with 1 mM EDTA, which impairs cell-cell adhesion by chelating calcium ions. Barrier integrity was measured from three donors (circles, squares and diamonds) in triplicate, across two independent experiments (colored gray and black). Loss of barrier integrity was demonstrated by a negative TEER change (**A**) and reduction in ZO-1 junctional complex protein total area normalised to number of 'in-focus' fields (**B**). For exemplar images see **Fig. S4**. Individual data points with treatment group means +/- 95% confidence intervals are plotted. Statistical analysis by general linear model with *p*-values: ***$p < 0.001$.

Supplementary Materials

Epithelial Barrier Integrity Profiling: Combined Approach Using Cellular Junctional Complex Imaging and Trans-Epithelial Electrical Resistance

Theresa J. Pell[1], Mike B. Gray[1], Sarah J. Hopkins[1], Richard Kasprowicz[1], James D. Porter[1], Tony Reeves[1], Wendy C. Rowan[1], Kuljit Singh[1], Ketil B. Tvermosegaard[1], Naheem Yaqub[2] and Gareth J. Wayne[1]

[1]GlaxoSmithKline R&D, Stevenage, Hertfordshire, SG1 2NY, UK

[2]University College London, London, NW3 2PF, UK

Corresponding author: Theresa J. Pell, GlaxoSmithKline R&D, Stevenage, Hertfordshire, SG1 2NY, UK. E-mail: theresa.j.pell@gsk.com

Materials and Methods

Materials

All reagents were from Sigma-Aldrich (Gillingham, Dorset, UK) unless otherwise stated. Dulbecco's Modified Eagle Medium (DMEM) used contained high glucose, GlutaMAX™ and sodium pyruvate (Gibco 31966; Thermo Fisher Scientific, Waltham MA).

Media Preparation

Bronchial Epithelial Growth Medium (BEGM™) containing 1:250 bovine pituitary extract (BPE), 1:1000 hydrocortisone, 0.5 ng/mL human epidermal growth factor (hEGF), 1:1000 epinephrine, 1:1000 transferrin, 0.0005% insulin, 1:1000 triiodothyronine, 0.003-5% gentamicin/amphotericin B (GA) and 500 µg/mL BSA (fatty acid free) was prepared by the addition of BEGM™ SingleQuots™ (CC-4175; Lonza, Basel, Switzerland), except retinoic acid, to filtered Bronchial Epithelial Basal Medium (BEBM™) (CC-3171; Lonza).

Small Airway Epithelial Cell Basal Medium (SABM™) Differentiation Medium containing 1:250 BPE, 1:1000 hydrocortisone, 0.5 ng/mL hEGF, 1:1000 epinephrine, 1:1000 transferrin, 0.0005% insulin, 1:1000 triiodothyronine and 0.003-5% GA was prepared as a 1:1 mix of DMEM:SABM™ (CC-3319; Lonza) which was filtered and then supplemented with Small Airway Epithelial Cell Growth Medium (SAGM™) SingleQuots™ (CC-4124; Lonza), except for retinoic acid.

BEBM™ Differentiation Medium containing 1:250 BPE, 1:1000 hydrocortisone, 0.5 ng/mL hEGF, 1:1000 epinephrine, 1:1000 transferrin, 0.0005% insulin, 1:1000 triiodothyronine and 0.003-5% GA was prepared as a 1:1 mix of DMEM:BEBM™, which was filtered and then supplemented with SAGM™ SingleQuots™ (CC-4124; Lonza), except for retinoic acid. Retinoic acid (R2625), dissolved to 10 mM in dimethylsulfoxide (DMSO), and then diluted to

50 µM in filtered 100% ethanol, was added to BEGM™ and SABM™/BEBM™ Differentiation Medium on the day of use, to a final concentration of 50 nM.

Lonza Human Bronchial Epithelial Cell Culture

Healthy non-smoker primary human bronchial epithelial cells (HBECs) (CC-2540; Lonza) were differentiated over 21 days at air-liquid interface (ALI) into a pseudostratified epithelium, following a method modified from Gray *et al*[1] using Clonetics™ Airway Epithelial Cell Systems (Lonza). HBECs were thawed, seeded into T75 cm^2 flasks in BEGM™ and cultured for 6-7 days at 37°C / 5% CO_2; media changing every 2-3 days.

The day before cell seeding into Transwell® permeable membrane support inserts (6.5 mm diameter, 0.4 µm pore size, polystyrene membrane; Costar 3470; Corning Life Sciences, Tewksbury, MA), the inserts were coated with human type IV collagen (C7521). A 2 mg/mL collagen stock solution was prepared in 0.25% acetic acid (Alfa Aesar 33252; Thermo Fisher Scientific), with shaking overnight at 4°C. A 0.15 µg/mL working solution of collagen was prepared in sterile water and filtered. Apical surfaces of the Transwell® inserts were coated with 50 µL/insert of 0.15 µg/mL collagen working solution and incubated overnight at room temperature in a sterile environment. Inserts were washed twice with 100 µL/insert of PBS pH7.4 without Ca^{2+}/Mg^{2+} (PBS -/-; D8537), the PBS was carefully aspirated, so as not to scratch the coating, to leave the inserts as dry as possible.

HBECs in flasks were washed with Hank's Buffered Salt Solution and lifted with Trypsin/0.025% ethylenediaminetetraacetic acid (EDTA) for 1.5 minutes at 37°C/5% CO_2, detachment was aided by firmly hitting the flask side (time in Trypsin/EDTA should be minimised). Trypsin was then neutralised with Trypsin Neutralizing Solution (ReagentPack™

Subculture Reagents CC-5034; Lonza). Cells were pelleted by centrifugation at 300 g for 5 minutes at room temperature and re-suspended to $1.25x10^6$ cells/mL in pre-warmed (37°C) BEGM™. HBECs (passage 3) were seeded at 75,000, 125,000 or 250,000 cells in 200 µL/Transwell® insert. 600 µL/well per-warmed BEGM™ was added to a 24-well receiver plate (Costar 3524; Corning Life Sciences) and the Transwell® inserts transferred to the receiver plate. Cells were cultured submerged for 2 days, to allow them to adhere to the membrane, and then air-lifted by removing the apical medium. Cells were differentiated at ALI for at least 21 days in 600 µL/well basolateral SABM™ Differentiation Medium; changing media and removing any apical mucus every 2-3 days.

Formation of the epithelium was monitored by Trans-Epithelial Electrical Resistance (TEER). For 250,000 cells/well ALI cultures, only wells with 0 h TEER readings $\geq 300\ \Omega.cm^2$, indicative of an intact epithelial barrier, were used for treatment. Wells seeded at lower seeding densities, to demonstrate effects on barrier integrity, were not excluded from experiments even if their TEER values were below $300\ \Omega.cm^2$.

Junctional Complex Immunostaining

Prior to fixation, HBEC ALI cultures grown in Transwell® inserts were gently washed three times with pre-warmed (37°C) filtered Phosphate Buffered Saline pH 7.4 supplemented with Ca^{2+}/Mg^{2+} (PBS) (Gibco 14040; Thermo Fisher Scientific). For the washes, volumes used were 1 mL/well in the basolateral well and 200 µL/well in the apical Transwell® insert, to remove mucus from the epithelial surface, which can hinder immunostaining. Cells were fixed with Parafix containing 4% paraformaldehyde (PRC/R/38/2; Pioneer Research Chemicals Ltd, Colchester, Essex, UK) for 15 minutes at room temperature (basolateral 600 µL/well, apical 200 µL/insert). Fixed cells were washed three times with PBS; the first wash was removed

immediately, and the remaining washes left 2 minutes each. Fixed cells for later immunostaining, were stored in sealed plates in PBS (basolateral: 600 µL/well, apical: 200 µL/insert) for up to one week at 4°C. PBS was removed from the basolateral and apical compartments, after which the apical surface of the cells was blocked and permeabilized with PBS containing 5% bovine serum albumin (BSA; A4503) and 0.5% Triton X-100 (T9284) for 1 h at room temperature (apical only: 200 µL/insert; basolateral well was left empty). Block-permeabilization solution was removed and primary antibodies were applied to the apical surface only (apical: 200 µL/insert; basolateral well was left empty): rabbit polyclonal antibody against zonula occludens-1 (ZO-1) (1:100, 2.5 µg/ml; Invitrogen 61-73000; Thermo Fisher Scientific) with or without mouse monoclonal antibody against occludin (1:100, 5 µg/ml; Invitrogen 33-1500; Thermo Fisher Scientific) in PBS containing 2% BSA and incubated, sealed, overnight at 4°C. The next day, the primary antibodies were aspirated, and the cells washed 5 times for 5 minutes each with PBS (apical only: 200 µL/insert). A cocktail of fluorescently conjugated anti-species secondary antibodies and nuclear counterstain was applied (apical only: 200 µL/insert): donkey anti-mouse Alexa Fluor® 488 (1:500, 4 µg/mL; Molecular Probes A-21202; ThermoFisher Scientific), donkey anti-rabbit Alexa Fluor® 647 (1:500, 4 µg/mL; Molecular Probes A-31573; Thermo Fisher Scientific) and Hoechst 33342 trihydrochloride (1.66 µM; Invitrogen H21492 dissolved in water to 2 mM; Thermo Fisher Scientific) in PBS containing 2% BSA (w/v) for 1 h at room temperature, protected from light. Cells were washed 5 times for 5 minutes each with PBS (apical only: 200 µL/insert) and then stored in PBS -/- (basolateral: 600 µL/well, apical: 200 µL/insert) at 4°C, protected from light, for up to one week until image acquisition.

Figures

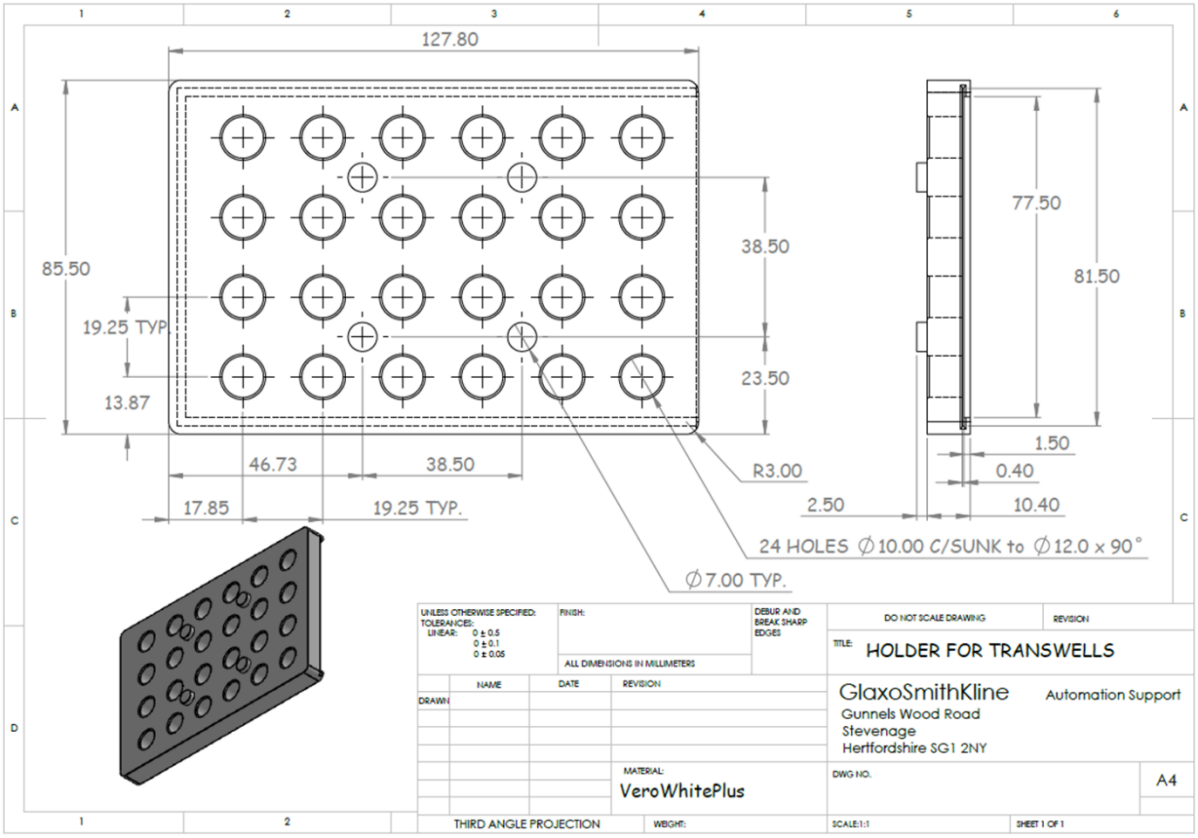

Figure S1. SOLIDWORKS® 2019 CAD designs for the 3D printed 24-well Transwell® insert holder, designed to the same footprint as a standard multi-well imaging plate, to ensure compatibility with automated high content imaging platforms. Dimensions are given in mm. SOLIDWORKS® CAD design files are available from the authors on request.

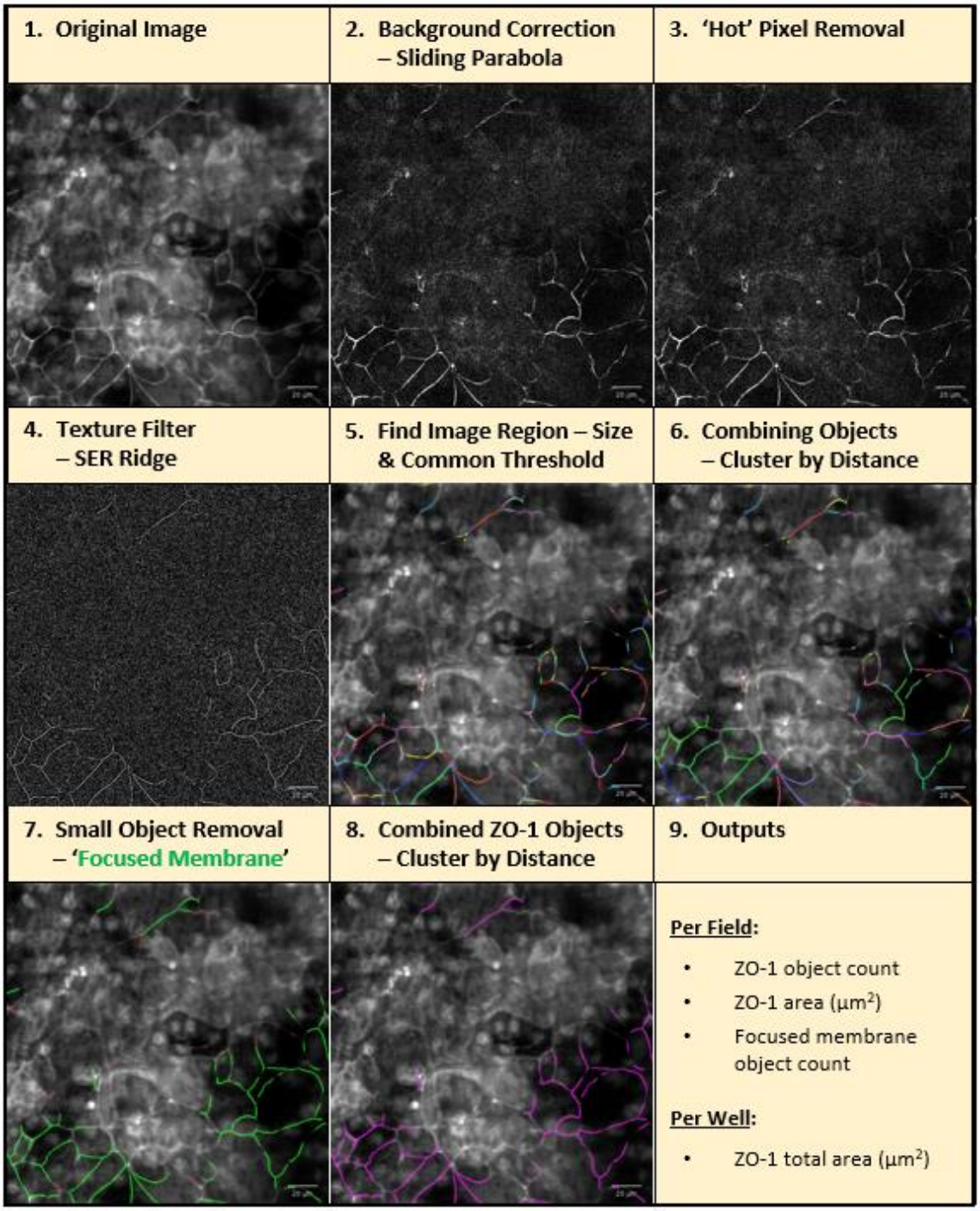

Figure S2. ZO-1 tight junction protein total area image analysis pipeline using Columbus™ v2.8.0 software (Perkin Elmer, Waltham, MA). The identical image analysis pipeline was used for occludin, except for optimisation of the background correction sliding parabola parameter (see **Tables S3-S4** for details). This analysis has the caveat that the same object can be counted in multiple planes, however, this error is consistent when the algorithm is only used to analyse epithelial layers of similar thicknesses. Exemplar images from ***Study 1, experiment 2:*** donor 1, 250000 cells/well treated daily for 72 h with vehicle control; plane 9 shown.

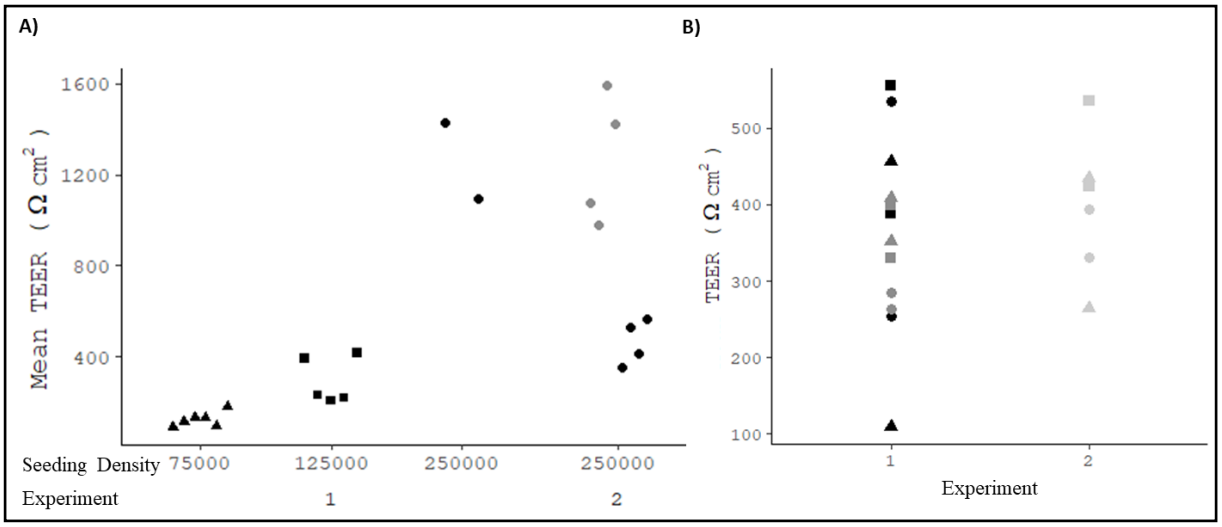

Figure S3. Barrier integrity of HBEC ALI cultures prior to treatment. 0 h mean TEER values are shown from triplicate technical reads from each well. (**A**) ***Study 1*** – two independent experiments using Lonza HBEC ALI cultures. *Experiment 1*: cells seeded at 75,000 (triangles), 125,000 (squares) and 250,000 cells/well (circles). *Experiment 2*: cells from two donors (colored black and gray) were seeded at 250,000 cells/well. (**B**) ***Study 2*** – three SmallAir™ HBEC donor ALI cultures (circles, squares and diamonds), performed in triplicate (replicate 1 in black, replicate 2 in dark gray and replicate three in light gray), across two independent experiments. No data points were excluded from downstream TEER change analyses.

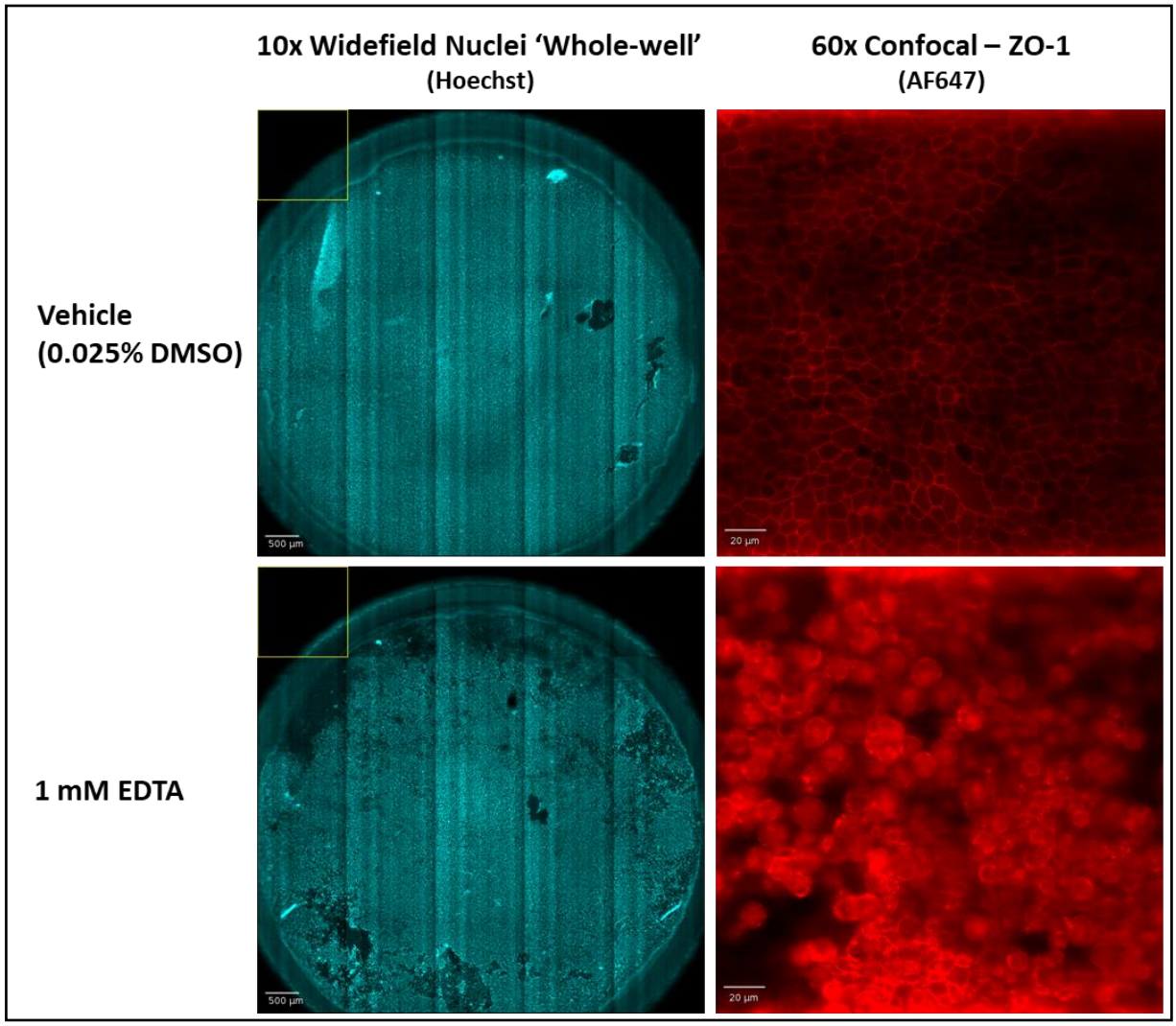

Figure S4. EDTA treatment altered ZO-1 tight junction protein pattern of staining. Representative 10x magnification widefield nuclei images of the 'whole well' and 60x magnification confocal images of ZO-1 tight junctional complex protein, showing single planes, from donor 1 (replicate 3) SmallAir™ HBEC ALI cultures. Cells were treated with vehicle control (0.025% DMSO) for 48 h or with 1 mM EDTA for the last 1 h. EDTA disruption of barrier integrity was demonstrated by a loss of ZO-1 'honeycomb' pattern of staining, indicative of an intact epithelial barrier.

Tables

Dye Channel	Imaging Target	Magnification	Mode	Excitation (nm)	Emission (nm)	Exposure (ms)
Hoechst	Nuclei	10x	Widefield 2D	405	455/50	200
Hoechst	Nuclei / FluoSpheres	60x	Widefield 2D	405	455/50	300
AF488	Occludin	60x	Confocal 3D	488	525/20	800
AF647	ZO-1	60x	Confocal 3D	642	706/72	400

Table S1. Image acquisition settings for the IN Cell Analyzer 6000 (Healthcare Life Sciences, Little Chalfont, Buckinghamshire, UK) high content imaging platform.

Image Analysis Pipeline	Population	Property
ZO-1	Modified Image Region_Threshold (2)	Number of Objects
	Modified Image Region_Threshold (2)	Region Area [pixel^2]
	Focused Membrane	Number of Objects
	Focused Membrane	Region Area [pixel^2]
	ZO-1	Area [µm^2]
	ZO-1 - Number of Objects	Object Count
	ZO-1 - Region Area [µm^2]	Sum per Well
	Focused Membrane - Number of Objects	Object Count
Occludin (Occ)	Modified Image Region_Threshold (2)	Number of Objects
	Modified Image Region_Threshold (2)	Region Area [pixel^2]
	Focused Membrane	Number of Objects
	Focused Membrane	Region Area [pixel^2]
	Occ	Area [µm^2]
	Occ - Number of Objects	Object Count
	Occ - Region Area [µm^2]	Sum per Well
	Focused Membrane - Number of Objects	Object Count

Table S2. Features measured in the junctional complex image analysis pipelines using Columbus™ v2.8.0 software. Parameters highlighted in gray were used to evaluate epithelial barrier integrity.

Input Image	**Stack Processing :** Individual Planes **Flatfield Correction :** None		
Filter Image	**Channel :** Cy5	**Method :** Sliding Parabola Curvature : 20	Output Image : Sliding Parabola
Calculate Image		**Method :** By Formula Formula : iif(A<5000, A, A.median) Channel A : Sliding Parabola Negative Values : Set to Zero Undefined Values : Set to Local Average	Output Image : Calc Image
Filter Image	**Channel :** Calc Image	**Method :** Texture SER Filter : SER Ridge Scale : 2 px Normalization by : Kernel	Output Image : SER Ridge (2)
Find Image Region	**Channel :** SER Ridge (2) **ROI :** None	**Method :** Common Threshold Threshold : 0.9 Split into Objects Area : > 40 px²	Output Population : Image Region_Threshold Output Region : Image Region_Threshold
Modify Population	**Population :** Image Region_Threshold **Region :** Image Region_Threshold	**Method :** Cluster by Distance Distance : 5 px Area : > 0 px²	Output Population : Modified Image Region_Threshold (2) Output Region : Region
Calculate Morphology Properties	**Population :** Modified Image Region_Threshold (2) **Region :** Region	**Method :** Standard Area Length	Output Properties : Region
Select Population	**Population :** Modified Image Region_Threshold (2)	**Method :** Filter by Property Region Area [px²] : > 75	Output Population : Focused Membrane
Calculate Morphology Properties	**Population :** Focused Membrane **Region :** Region	**Method :** Standard Area	Output Properties : Modified Selected Membrane
Modify Population	**Population :** Focused Membrane **Region :** Region	**Method :** Cluster by Distance Distance : 500 px Area : > 1000 px²	Output Population : ZO-1 Output Region : Region
Calculate Morphology Properties	**Population :** ZO-1 **Region :** Region	**Method :** Standard Area	Output Properties : Region
Define Results	**Method :** Standard Output ZO-1 - Number of Objects : Object Count Output Name : ZO-1 Objects **Method :** Standard Output ZO-1 - Region Area [µm²] : Sum Output Name : ZO-1 Area [µm²] - Sum per Well **Method :** Standard Output Focused Membrane - Number of Objects : Object Count Output Name : Focused Objects **Population : Modified Image Region_Threshold (2) :** None Population : Image Region_Threshold : None Population : Focused Membrane : None Population : ZO-1 : ALL		

Table S3. ZO-1 image analysis pipeline extracted from Columbus™ software.

Input Image	**Stack Processing :** Individual Planes **Flatfield Correction :** None		
Filter Image	**Channel :** FITC	**Method :** Sliding Parabola Curvature : 1	Output Image : Sliding Parabola
Calculate Image		**Method :** By Formula Formula : iif(A<5000, A, A.median) Channel A : Sliding Parabola Negative Values : Set to Zero Undefined Values : Set to Local Average	Output Image : Calc Image
Filter Image	**Channel :** Calc Image	**Method :** Texture SER Filter : SER Ridge Scale : 2 px Normalization by : Kernel	Output Image : SER Ridge (2)
Find Image Region	**Channel :** SER Ridge (2) **ROI :** None	**Method :** Common Threshold Threshold : 0.9 Split into Objects Area : > 40 px²	Output Population : Image Region_Threshold Output Region : Image Region_Threshold
Modify Population	**Population :** Image Region_Threshold **Region :** Image Region_Threshold	**Method :** Cluster by Distance Distance : 5 px Area : > 0 px²	Output Population : Modified Image Region_Threshold (2) Output Region : Region
Calculate Morphology Properties	**Population :** Modified Image Region_Threshold (2) **Region :** Region	**Method :** Standard Area Length	Output Properties : Region
Select Population	**Population :** Modified Image Region_Threshold (2)	**Method :** Filter by Property Region Area [px²] : > 75	Output Population : Focused Membrane
Calculate Morphology Properties	**Population :** Focused Membrane **Region :** Region	**Method :** Standard Area	Output Properties : Modified Selected Membrane
Modify Population	**Population :** Focused Membrane **Region :** Region	**Method :** Cluster by Distance Distance : 500 px Area : > 1000 px²	Output Population : Occ Output Region : Region
Calculate Morphology Properties	**Population :** Occ **Region :** Region	**Method :** Standard Area	Output Properties : Region
Define Results	**Method :** Standard Output Occ - Number of Objects : Object Count Output Name : Occ Objects **Method :** Standard Output Occ - Region Area [µm²] : Sum Output Name : Occ Area [µm²] - Sum per Well **Method :** Standard Output Focused Membrane - Number of Objects : Object Count Output Name : Focused Objects **Population : Modified Image Region_Threshold (2) :** None Population : Image Region_Threshold : None Population : Focused Membrane : None Population : Occ : ALL		

Table S4. Occludin image analysis pipeline extracted from Columbus™ software.

Stimulus	Plate ID	Well ID	Donor	Cells/Well	Incubation Time	Mean TEER ($\Omega.cm^2$)	Log10(Mean TEER)	TEER Change	Expt
Vehicle	1	C1	1	250000	0 h	1429.9	3.16		1
Vehicle	1	C2	1	125000	0 h	392.4	2.59		1
Vehicle	1	C3	1	75000	0 h	88.6	1.95		1
TGF-β1	1	D1	1	250000	0 h	1092.1	3.04		1
TGF-β1	1	D2	1	125000	0 h	230.2	2.36		1
TGF-β1	1	D3	1	75000	0 h	113.4	2.05		1
TGF-β1	1	D4	1	75000	0 h	129.8	2.11		1
Vehicle	2	A1	1	125000	0 h	205.0	2.31		1
Vehicle	2	A2	1	75000	0 h	129.5	2.11		1
TGF-β1	2	B1	1	125000	0 h	218.5	2.34		1
TGF-β1	2	B2	1	75000	0 h	92.5	1.97		1
TGF-β1	2	C1	1	125000	0 h	415.3	2.62		1
TGF-β1	2	C2	1	75000	0 h	180.8	2.26		1
Vehicle	1	C1	1	250000	72 h	384.2	2.58	-0.57	1
Vehicle	1	C2	1	125000	72 h	297.8	2.47	-0.12	1
Vehicle	1	C3	1	75000	72 h	94.3	1.97	0.03	1
TGF-β1	1	D1	1	250000	72 h	81.5	1.91	-1.13	1
TGF-β1	1	D2	1	125000	72 h	66.6	1.82	-0.54	1
TGF-β1	1	D3	1	75000	72 h	73.8	1.87	-0.19	1
TGF-β1	1	D4	1	75000	72 h	56.8	1.75	-0.36	1
Vehicle	2	A1	1	125000	72 h	142.5	2.15	-0.16	1
Vehicle	2	A2	1	75000	72 h	163.7	2.21	0.10	1
TGF-β1	2	B1	1	125000	72 h	69.3	1.84	-0.50	1
TGF-β1	2	B2	1	75000	72 h	72.8	1.86	-0.10	1
TGF-β1	2	C1	1	125000	72 h	70.3	1.85	-0.77	1
TGF-β1	2	C2	1	75000	72 h	73.2	1.86	-0.39	1
Vehicle	1	A1	1	250000	0 h	350.2	2.54		2
Vehicle	1	A2	1	250000	0 h	530.1	2.72		2
TGF-β1	1	A3	1	250000	0 h	410.9	2.61		2
TGF-β1	1	A4	1	250000	0 h	562.3	2.75		2
Vehicle	1	B1	2	250000	0 h	1073.4	3.03		2
Vehicle	1	B2	2	250000	0 h	981.0	2.99		2
TGF-β1	1	B3	2	250000	0 h	1592.0	3.20		2
TGF-β1	1	B4	2	250000	0 h	1425.3	3.15		2
Vehicle	1	A1	1	250000	24 h	625.9	2.80	0.25	2
Vehicle	1	A2	1	250000	24 h	887.9	2.95	0.22	2
TGF-β1	1	A3	1	250000	24 h	295.8	2.47	-0.14	2
TGF-β1	1	A4	1	250000	24 h	317.2	2.50	-0.25	2
Vehicle	1	B1	2	250000	24 h	1816.3	3.26	0.23	2
Vehicle	1	B2	2	250000	24 h	1663.9	3.22	0.23	2
TGF-β1	1	B3	2	250000	24 h	180.5	2.26	-0.95	2
TGF-β1	1	B4	2	250000	24 h	150.0	2.18	-0.98	2
Vehicle	1	A1	1	250000	48 h	618.6	2.79	0.25	2
Vehicle	1	A2	1	250000	48 h	884.7	2.95	0.22	2
TGF-β1	1	A3	1	250000	48 h	126.9	2.10	-0.51	2
TGF-β1	1	A4	1	250000	48 h	129.7	2.11	-0.64	2
Vehicle	1	B1	2	250000	48 h	1748.7	3.24	0.21	2
Vehicle	1	B2	2	250000	48 h	1354.3	3.13	0.14	2
TGF-β1	1	B3	2	250000	48 h	91.0	1.96	-1.24	2
TGF-β1	1	B4	2	250000	48 h	88.1	1.95	-1.21	2
Vehicle	1	A1	1	250000	72 h	405.8	2.61	0.06	2
Vehicle	1	A2	1	250000	72 h	753.6	2.88	0.15	2
TGF-β1	1	A3	1	250000	72 h	88.0	1.94	-0.67	2
TGF-β1	1	A4	1	250000	72 h	77.6	1.89	-0.86	2
Vehicle	1	B1	2	250000	72 h	976.8	2.99	-0.04	2
Vehicle	1	B2	2	250000	72 h	1035.1	3.01	0.02	2
TGF-β1	1	B3	2	250000	72 h	70.7	1.85	-1.35	2
TGF-β1	1	B4	2	250000	72 h	68.9	1.84	-1.32	2

Table S5. ***Study 1*** – TEER values. Log10 transformation and TEER change [log10(mean $TEER_t$)-log10(mean $TEER_0$)] calculated from TEER data generated in two independent experiments (Expt), to investigate the effects of seeding density and TGF-β treatment on barrier integrity.

Stimulus	Well ID	Donor	Cells/Well	Junction Protein	Total Region Area (µm²)	√[Total Region Area] (√µm²)	Expt
Vehicle	C1	1	250000	ZO-1	11156	105.6	1
TGF-β	D1	1	250000	ZO-1	2065	45.4	1
Vehicle	C2	1	125000	ZO-1	9146	95.6	1
TGF-β	D2	1	125000	ZO-1	1172	34.2	1
Vehicle	C3	1	75000	ZO-1	3765	61.4	1
TGF-β	D3	1	75000	ZO-1	476	21.8	1
TGF-β	D4	1	75000	ZO-1	1458	38.2	1
Vehicle	C1	1	250000	Occludin	15014	122.5	1
TGF-β	D1	1	250000	Occludin	2511	50.1	1
Vehicle	C2	1	125000	Occludin	9081	95.3	1
TGF-β	D2	1	125000	Occludin	977	31.2	1
Vehicle	C3	1	75000	Occludin	4169	64.6	1
TGF-β	D3	1	75000	Occludin	790	28.1	1
TGF-β	D4	1	75000	Occludin	1619	40.2	1
Vehicle	B2	2	250000	ZO-1	18467	135.9	2
TGF-β	B4	2	250000	ZO-1	1449	38.1	2
Vehicle	A2	1	250000	ZO-1	13942	118.1	2
TGF-β	A4	1	250000	ZO-1	2638	51.4	2
Vehicle	B1	2	250000	ZO-1	10432	102.1	2
TGF-β	B3	2	250000	ZO-1	572	23.9	2
Vehicle	A1	1	250000	ZO-1	15849	125.9	2
TGF-β	A3	1	250000	ZO-1	2055	45.3	2
Vehicle	B1	2	250000	Occludin	14335	119.7	2
TGF-β	B3	2	250000	Occludin	1528	39.1	2
Vehicle	A1	1	250000	Occludin	17447	132.1	2
TGF-β	A3	1	250000	Occludin	3060	55.3	2

Table S6. ***Study 1*** – ZO-1 and occludin junctional complex protein total area. Data from two independent experiments, to investigate the effects of seeding density and TGF-β treatment on barrier integrity.

Stimulus	Plate ID	Well ID	Donor	Replicate	Stimulus Time	Incubation Time	TEER (Ω.cm	Log10 (TEER)	TEER Change	Expt
Vehicle	1	D1	1	1	48 h	0 h	535.5	2.73		1
Vehicle	1	D2	2	1	48 h	0 h	456.3	2.66		1
Vehicle	1	D3	3	1	48 h	0 h	556.1	2.75		1
EDTA	1	D4	1	1	1 h	0 h	253.5	2.40		1
EDTA	1	D5	2	1	1 h	0 h	108.8	2.04		1
EDTA	1	D6	3	1	1 h	0 h	388.7	2.59		1
Vehicle	2	D1	1	2	48 h	0 h	284.5	2.45		1
Vehicle	2	D2	2	2	48 h	0 h	408.0	2.61		1
Vehicle	2	D3	3	2	48 h	0 h	398.8	2.60		1
EDTA	2	D4	1	2	1 h	0 h	263.6	2.42		1
EDTA	2	D5	2	2	1 h	0 h	351.3	2.55		1
EDTA	2	D6	3	2	1 h	0 h	330.3	2.52		1
Vehicle	1	D1	1	1	48 h	48 h	329.8	2.52	-0.21	1
Vehicle	1	D2	2	1	48 h	48 h	434.2	2.64	-0.02	1
Vehicle	1	D3	3	1	48 h	48 h	399.5	2.60	-0.14	1
EDTA	1	D4	1	1	1 h	1 h	70.3	1.85	-0.56	1
EDTA	1	D5	2	1	1 h	1 h	72.2	1.86	-0.18	1
EDTA	1	D6	3	1	1 h	1 h	72.2	1.86	-0.73	1
Vehicle	2	D1	1	2	48 h	48 h	331.4	2.52	0.07	1
Vehicle	2	D2	2	2	48 h	48 h	306.1	2.49	-0.12	1
Vehicle	2	D3	3	2	48 h	48 h	358.7	2.55	-0.05	1
EDTA	2	D4	1	2	1 h	1 h	59.9	1.78	-0.64	1
EDTA	2	D5	2	2	1 h	1 h	63.8	1.80	-0.74	1
EDTA	2	D6	3	2	1 h	1 h	60.9	1.78	-0.73	1
Vehicle	1	D1	1	3	48 h	0 h	331.5	2.52		2
Vehicle	1	D2	2	3	48 h	0 h	264.4	2.42		2
Vehicle	1	D3	3	3	48 h	0 h	423.6	2.63		2
EDTA	1	D4	1	3	1 h	0 h	393.3	2.59		2
EDTA	1	D5	2	3	1 h	0 h	434.3	2.64		2
EDTA	1	D6	3	3	1 h	0 h	536.1	2.73		2
Vehicle	1	D1	1	3	48 h	48 h	401.3	2.60	0.08	2
Vehicle	1	D2	2	3	48 h	48 h	238.2	2.38	-0.05	2
Vehicle	1	D3	3	3	48 h	48 h	439.5	2.64	0.02	2
EDTA	1	D4	1	3	1 h	1 h	72.3	1.86	-0.74	2
EDTA	1	D5	2	3	1 h	1 h	78.1	1.89	-0.75	2
EDTA	1	D6	3	3	1 h	1 h	76.0	1.88	-0.85	2

Table S7. ***Study 2*** – TEER values. Log10 transformation and TEER change [log10($TEER_t$)-log10($TEER_0$)] calculated from TEER data generated in two independent experiments, to investigate the effects of EDTA treatment on barrier integrity.

Stimulus	Plate ID	Well ID	Donor	Replicate	Stimulus Time	No. of In-Focus Fields	ZO-1 Total Region Area (µm²)	√[ZO-1 Total Region Area] (√µm²)	√[ZO-1 Total Region Area] / No. of In-Focus Fields (√µm²)	Expt
Vehicle	1	D1	1	1	48 h	6	47403	217.7	36.3	1
Vehicle	1	D2	2	1	48 h	6	46069	214.6	35.8	1
Vehicle	1	D3	3	1	48 h	6	27906	167.1	27.8	1
EDTA	1	D4	1	1	1 h	6	6714	81.9	13.7	1
EDTA	1	D5	2	1	1 h	6	3117	55.8	9.3	1
EDTA	1	D6	3	1	1 h	6	2926	54.1	9.0	1
Vehicle	2	D1	1	2	48 h	6	50512	224.7	37.5	1
Vehicle	2	D2	2	2	48 h	6	45504	213.3	35.6	1
Vehicle	2	D3	3	2	48 h	6	31770	178.2	29.7	1
EDTA	2	D4	1	2	1 h	6	11198	105.8	17.6	1
EDTA	2	D5	2	2	1 h	6	4098	64.0	10.7	1
EDTA	2	D6	3	2	1 h	6	6810	82.5	13.8	1
Vehicle	3	D1	1	3	48 h	6	50012	223.6	37.3	2
Vehicle	3	D2	2	3	48 h	6	39554	198.9	33.1	2
Vehicle	3	D3	3	3	48 h	6	29946	173.0	28.8	2
EDTA	3	D4	1	3	1 h	6	10380	101.9	17.0	2
EDTA	3	D5	2	3	1 h	6	11289	106.2	17.7	2
EDTA	3	D6	3	3	1 h	5	8739	93.5	18.7	2

Table S8. ***Study 2*** – ZO-1 junctional complex protein total area. Data from two independent experiments, to investigate the effects of EDTA treatment on barrier integrity.

Fig.	Donor	Cells/ Well	Stimulus	Time	Group Mean Parameter	Group Mean Value	SE	Degrees of Freedom	Lower CL	Upper CL
4A	1	75000	Untreated	0 h	log10(mean TEER)	2.0751	0.0515	10	1.9603	2.1900
	1	125000	Untreated	0 h	log10(mean TEER)	2.4451	0.0565	10	2.3193	2.5709
	1	250000	Untreated	0 h	log10(mean TEER)	3.0968	0.0893	10	2.8979	3.2957
4C	1	75000	Vehicle	72 h	TEER Change	0.0645	0.0867	4	-0.1761	0.3051
	1	75000	TGF-ß1	72 h	TEER Change	-0.2607	0.0613	4	-0.4309	-0.0905
	1	125000	Vehicle	72 h	TEER Change	-0.1390	0.0857	3	-0.4118	0.1338
	1	125000	TGF-ß1	72 h	TEER Change	-0.6030	0.0700	3	-0.8258	-0.3803
4E	2	250000	Vehicle	24 h	TEER Change	0.2300	0.0295	4	0.1482	0.3118
	1	250000	Vehicle	24 h	TEER Change	0.2350	0.0295	4	0.1532	0.3168
	2	250000	TGF-ß1	24 h	TEER Change	-0.9650	0.0295	4	-1.0468	-0.8832
	1	250000	TGF-ß1	24 h	TEER Change	-0.1950	0.0295	4	-0.2768	-0.1132
	2	250000	Vehicle	48 h	TEER Change	0.1750	0.0384	4	0.0684	0.2816
	1	250000	Vehicle	48 h	TEER Change	0.2350	0.0384	4	0.1284	0.3416
	2	250000	TGF-ß1	48 h	TEER Change	-1.2250	0.0384	4	-1.3316	-1.1184
	1	250000	TGF-ß1	48 h	TEER Change	-0.5750	0.0384	4	-0.6816	-0.4684
	2	250000	Vehicle	72 h	TEER Change	-0.0100	0.0552	4	-0.1632	0.1432
	1	250000	Vehicle	72 h	TEER Change	0.1050	0.0552	4	-0.0482	0.2582
	2	250000	TGF-ß1	72 h	TEER Change	-1.3350	0.0552	4	-1.4882	-1.1818
	1	250000	TGF-ß1	72 h	TEER Change	-0.7650	0.0552	4	-0.9182	-0.6118
4F	1	250000	Vehicle	72 h	Square Root of ZO-1 Total Region Area	120.50	6.41	5	104.02	136.98
	1	250000	TGF-ß1	72 h	Square Root of ZO-1 Total Region Area	39.67	6.41	5	23.19	56.15

Table S9. ***Study 1*** – summary group mean and confidence limit (CL) data used to plot **Fig. 4**. Confidence intervals from two independent experiments, to investigate the effects of seeding density and TGF-β treatment on barrier integrity

Figure	Stimulus	Group Mean Parameter	Group Mean Value	SE	Degrees of Freedom	Lower CL	Upper CL
5A	Vehicle	TEER Change	-0.0474	0.0552	12	-0.1677	0.0730
	EDTA	TEER Change	-0.6571	0.0552	12	-0.7775	-0.5368
5B	Vehicle	Square Root of ZO-1 Total Region Area / In-focus Fields	82.16	2.3068	12	77.14	87.19
	EDTA	Square Root of ZO-1 Total Region Area / In-focus Fields	34.24	2.3068	12	29.21	39.26

Table S10. ***Study 2*** – **s**ummary group mean and confidence limit data used to plot **Fig. 5**. Confidence intervals from two independent experiments, to investigate the effects of EDTA treatment on barrier integrity

Figure	Contrast	Estimate	SE	Degrees of Freedom	t Ratio	*p*-Value	Significance Level	Lower CL	Upper CL
4A	125K vs 75K	0.37	0.0765	10	4.84	6.83E-04	***	0.1996	0.5403
	250K vs 125K	0.65	0.1056	10	6.17	1.06E-04	***	0.4163	0.8871
4C	75K: TGFb vs Vehicle	-0.33	0.1057	7	-3.08	1.79E-02	*	-0.5750	-0.0754
	125K: TGFb vs Vehicle	-0.46	0.1114	7	-4.17	4.21E-03	**	-0.7274	-0.2007
4E	24 h, donor 1: TGFb vs Vehicle	-0.43	0.0417	4	-10.32	4.98E-04	***	-0.5457	-0.3143
	24 h, donor 2: TGFb vs Vehicle	-1.20	0.0417	4	-28.67	8.81E-06	***	-1.3107	-1.0793
	48 h, donor 1: TGFb vs Vehicle	-0.81	0.0543	4	-14.91	1.18E-04	***	-0.9608	-0.6592
	48 h, donor 2: TGFb vs Vehicle	-1.40	0.0543	4	-25.78	1.35E-05	***	-1.5508	-1.2492
	72 h, donor 1: TGFb vs Vehicle	-0.87	0.0780	4	-11.15	3.68E-04	***	-1.0866	-0.6534
	72 h, donor 2: TGFb vs Vehicle	-1.33	0.0780	4	-16.98	7.05E-05	***	-1.5416	-1.1084

Table S11. ***Study 1*** – one-way ANOVA statistical analyses to test whether TEER changes from baseline for wells with reduced seeding density or TGF-β1 treatment were significantly different to the change from baseline for vehicle controls. A separate one-way ANOVA was used for each treatment-control comparison and each timepoint. *p*-values: *$p<0.05$; **$p<0.01$; ***$p<0.001$

Figure		Degrees of Freedom	Sum Square	Mean Square	F Value	p-Value	Significance Level
4F	Stimulus	1	2.7115	2.7115	99.67	3.63E-06	***
	Residuals	9	0.2448	0.0272	#N/A	#N/A	
5A	Stimulus	1	1.6731	1.6731	60.93	4.83E-06	***
	Residuals	12	0.3295	0.0275	#N/A	#N/A	
5B	Stimulus	1	2.7610	2.7610	123.85	1.11E-07	***
	Residuals	12	0.2675	0.0223	#N/A	#N/A	

Table S12. Statistical analyses using general linear models. ***Study 1*** – to test whether ZO-1 tight junction total protein area changes from baseline, following TGF-β1 treatment (**Fig. 4F**), were significantly different to the change from baseline for vehicle controls, a general linear model was fitted with two fixed effects: treatment and donor. ***Study 2*** – to test whether TEER (**Fig. 5A**) or ZO-1 total area (**Fig. 5B**) changes from baseline, following EDTA treatment, were significantly different to the change from baseline for vehicle controls, general linear models were fitted with three fixed effects: treatment, HBEC donor and assay plate. *p*-values: ***$p < 0.001$.

References

1. Gray, T. E.; Guzman, K.; Davis, C. W.; et al. Mucociliary Differentiation of Serially Passaged Normal Human Tracheobronchial Epithelial Cells. *Am. J. Respir. Cell Mol. Biol.* **1996,** *14*, 104-12.